

# Bilinear Pooling in video-QA: Empirical challenges and motivational drift from neurological parallels

Thomas Winterbottom <sup>Corresp., 1</sup>, Sarah Xiao <sup>2</sup>, Alistair McLean <sup>3</sup>, Noura Al Moubayed <sup>1</sup>

<sup>1</sup> Department of Computer Science, Durham University, Durham, United Kingdom

<sup>2</sup> Durham University Business School, Durham University, Durham, Durham, United Kingdom

<sup>3</sup> Carbon AI, Middlesbrough, United Kingdom

Corresponding Author: Thomas Winterbottom

Email address: thomas.i.winterbottom@durham.ac.uk

Bilinear pooling (BLP) refers to a family of operations recently developed for fusing features from different modalities predominantly for visual question answering (VQA) models. Successive BLP techniques have yielded higher performance with lower computational expense, yet at the same time they have drifted further from the original motivational justification of bilinear models, instead becoming empirically motivated by task performance. Furthermore, despite significant success in text-image fusion in VQA, BLP has not yet gained such notoriety in video-QA. Though BLP methods have continued to perform well on video tasks when fusing vision and non-textual features, BLP has recently been overshadowed by other vision and textual feature fusion techniques in video-QA. We aim to add a new perspective to the empirical and motivational drift in BLP. We take a step back and discuss the motivational origins of BLP, highlighting the often-overlooked parallels to neurological theories (Dual Coding Theory and The Two-Stream Model of Vision). We seek to carefully and experimentally ascertain the empirical strengths and limitations of BLP as a multimodal text-vision fusion technique in video-QA using 2 models (TVQA baseline and heterogeneous-memory-enhanced 'HME' model) and 4 datasets (TVQA, TGif-QA, MSVD-QA, and EgoVQA). We examine the impact of both simply replacing feature concatenation in the existing models with BLP, and a modified version of the TVQA baseline to accommodate BLP that we name the 'dual-stream' model. We find that our relatively simple integration of BLP does not increase, and mostly harms, performance on these video-QA benchmarks. Using our insights on recent work in BLP for video-QA results and recently proposed theoretical multimodal fusion taxonomies, we offer insight into why BLP-driven performance gain for video-QA benchmarks may be more difficult to achieve than in earlier VQA models. We both share our perspective on, and suggest solutions for, the key issues we identify with BLP techniques for multimodal fusion in video-QA. We look beyond the empirical justification of BLP techniques and propose both alternatives and

improvements to multimodal fusion by drawing neurological inspiration from Dual Coding Theory and the Two-Stream Model of Vision. We qualitatively highlight the potential for neurological inspirations in video-QA by identifying the relative abundance of psycholinguistically 'concrete' words in the vocabularies for each of the text components (e.g. questions and answers) of the 4 video-QA datasets we experiment with.

# 1 Bilinear Pooling in Video-QA: Empirical 2 Challenges and Motivational Drift from 3 Neurological Parallels

4 Thomas Winterbottom<sup>1</sup>, Sarah Xiao<sup>2</sup>, Alistair McLean<sup>3</sup>, and Noura Al  
5 Moubayed<sup>1</sup>

6 <sup>1</sup>Department of Computer Science, Durham University

7 <sup>2</sup>Durham University Business School

8 <sup>3</sup>Carbon AI, United Kingdom

9 Corresponding author:

10 Thomas Winterbottom<sup>1</sup>

11 Email address: thomas.i.winterbottom@durham.ac.uk

## 12 ABSTRACT

13 Bilinear pooling (BLP) refers to a family of operations recently developed for fusing features from different  
14 modalities predominantly for visual question answering (VQA) models. Successive BLP techniques  
15 have yielded higher performance with lower computational expense, yet at the same time they have  
16 drifted further from the original motivational justification of bilinear models, instead becoming empirically  
17 motivated by task performance. Furthermore, despite significant success in text-image fusion in VQA,  
18 BLP has not yet gained such notoriety in video-QA. Though BLP methods have continued to perform  
19 well on video tasks when fusing vision and *non-textual* features, BLP has recently been overshadowed  
20 by other vision and *textual* feature fusion techniques in video-QA. We aim to add a new perspective to  
21 the empirical and motivational drift in BLP. We take a step back and discuss the motivational origins  
22 of BLP, highlighting the often-overlooked parallels to neurological theories (Dual Coding Theory and  
23 The Two-Stream Model of Vision). We seek to carefully and experimentally ascertain the empirical  
24 strengths and limitations of BLP as a multimodal text-vision fusion technique in video-QA using 2 models  
25 (TVQA baseline and heterogeneous-memory-enhanced 'HME' model) and 4 datasets (TVQA, TGif-QA,  
26 MSVD-QA, and EgoVQA). We examine the impact of both simply replacing feature concatenation in the  
27 existing models with BLP, and a modified version of the TVQA baseline to accommodate BLP that we  
28 name the 'dual-stream' model. We find that our relatively simple integration of BLP does not increase,  
29 and mostly harms, performance on these video-QA benchmarks. Using our insights on recent work in  
30 BLP for video-QA results and recently proposed theoretical multimodal fusion taxonomies, we offer insight  
31 into why BLP-driven performance gain for video-QA benchmarks may be more difficult to achieve than in  
32 earlier VQA models. We both share our perspective on, and suggest solutions for, the key issues we  
33 identify with BLP techniques for multimodal fusion in video-QA. We look beyond the empirical justification  
34 of BLP techniques and propose both alternatives and improvements to multimodal fusion by drawing  
35 neurological inspiration from Dual Coding Theory and the Two-Stream Model of Vision. We qualitatively  
36 highlight the potential for neurological inspirations in video-QA by identifying the relative abundance of  
37 psycholinguistically 'concrete' words in the vocabularies for each of the text components (e.g. questions  
38 and answers) of the 4 video-QA datasets we experiment with.

## 39 INTRODUCTION

40 To solve the growing abundance of complex deep learning tasks, it is essential to develop modelling  
41 and learning strategies with the capacity to learn complex and nuanced multimodal relationships and  
42 representations. To this end, research efforts in multimodal deep learning have taken aim at the relationship  
43 between vision and text through visual question answering (VQA) Wu et al. (2017); Srivastava et al.  
44 (2020) and more recently video question answering (video-QA) Sun et al. (2021). A particularly notorious  
45 solution to learning multimodal relationships in VQA is the family of bilinear pooling (BLP) operators  
46 Gao et al. (2016); Kim et al. (2017); Yu et al. (2017); Ben-younes et al. (2017); Yu et al. (2018b);

47 Ben-Younes et al. (2019). A bilinear (outer product) expansion is thought to encourage models to learn  
48 interactions between two feature spaces and has experimentally outperformed ‘simpler’ vector operations  
49 (i.e. concatenation and element-wise-addition/multiplication) on VQA benchmarks. Though successive  
50 BLP techniques focus on leveraging higher performance with lower computational expense, which we  
51 wholeheartedly welcome, the context of their use has subtly drifted from application in earlier bilinear  
52 models e.g. where in Lin et al. (2015) the bilinear mapping is learned between convolution maps (a  
53 tangible and visualisable parameter), from compact BLP Gao et al. (2016) onwards the bilinear mapping  
54 is learned between indexes of deep feature vectors (a much less tangible unit of representation). Though  
55 such changes are not necessarily problematic and the improved VQA performance they have yielded is  
56 valuable, they represent a broader trend of the use of BLP methods in multimodal fusion being justified  
57 *only* by empirical success. Furthermore, despite BLP’s history of success in text-image fusion in VQA, it  
58 has not yet gained such notoriety in video-QA. Though BLP methods have continued to perform well  
59 on video tasks when fusing vision and *non-textual* features Hu et al. (2021); Zhou et al. (2021); Pang  
60 et al. (2021); Xu et al. (2021); Deng et al. (2021); Wang et al. (2021); Deb et al. (2022); Sudhakaran  
61 et al. (2021), BLP has recently been overshadowed by other vision and *textual* feature fusion techniques  
62 in video-QA Kim et al. (2019); Li et al. (2019); Gao et al. (2019); Liu et al. (2021); Liang et al. (2019).  
63 In this paper, we aim to add a new perspective to the empirical and motivational drift in BLP. Our  
64 contributions include the following: **I**) We carefully and experimentally ascertain the empirical strengths  
65 and limitations of BLP as a multimodal text-vision fusion technique on 2 models (TVQA baseline and  
66 heterogeneous-memory-enhanced ‘HME’ model) and 4 datasets (TVQA, TGif-QA, MSVD-QA and  
67 EgoVqa). To this end, our experiments include replacing feature concatenation in the existing models with  
68 BLP, and a modified version of the TVQA baseline to accommodate BLP that we name the ‘dual-stream’  
69 model. Furthermore, we contrast BLP (classified as a ‘joint’ representation by Baltrušaitis et al. (2019))  
70 with deep canonical cross correlation (a ‘co-ordinated representation’). We find that our relatively simple  
71 integration of BLP does not increase, and mostly harms, performance on these video-QA benchmarks. **II**)  
72 We discuss the motivational origins of BLP and share our observations of bilinearity in text-vision fusion.  
73 **III**) By observing trends in recent work using BLP for multimodal video tasks and recently proposed  
74 theoretical multimodal fusion taxonomies, we offer insight into why BLP-driven performance gain for  
75 video-QA benchmarks may be more difficult to achieve than in earlier VQA models. **IV**) We identify  
76 temporal alignment and inefficiency (computational resources *and* performance) as key issues with BLP  
77 as a multimodal text-vision fusion technique in video-QA, and highlight concatenation and attention  
78 mechanisms as an ideal alternative. **V**) In parallel with the *empirically justified* innovations driving BLP  
79 methods, we explore the often-overlooked similarities of bilinear and multimodal fusion to neurological  
80 theories e.g. Dual Coding Theory Paivio (2013, 2014) and the Two-Stream Model of Vision Goodale  
81 and Milner (1992); Milner (2017), and propose several potential *neurologically justified* alternatives  
82 and improvements to existing text-image fusion. We highlight the latent potential already in existing  
83 video-QA dataset to exploit neurological theories by presenting a qualitative analysis of occurrence of  
84 psycholinguistically ‘concrete’ words in the vocabularies of the textual components of the 4 video-QA we  
85 experiment with.

## 86 **BACKGROUND: BILINEAR POOLING**

87 In this section we outline the development of BLP techniques, highlight how bilinear models parallel the  
88 two-stream model of vision, and discuss where bilinear models diverged from their original motivation.

### 89 **Concatenation**

90 Early works use Vector concatenation to project different features into a new joint feature space. Zhou  
91 et al. (2015) use vector concatenation on the CNN image and text features in their simple baseline VQA  
92 model. Similarly, Lu et al. (2016) concatenate image attention and textual features. Vector concatenation  
93 is a projection of both input vectors into a new ‘joint’ dimensional space. Vector concatenation as  
94 a multimodal feature fusion technique in VQA is considered a baseline and is generally empirically  
95 outperformed in VQA by the following bilinear techniques.

### 96 **Bilinear Models**

97 Working from the observations that “perceptual systems routinely separate ‘content’ from ‘style’”, Tenen-  
98 baum and Freeman (2000) proposed a bilinear framework on these two different aspects of purely visual

99 inputs. They find that the multiplicative bilinear model provides “sufficiently expressive representations  
100 of factor interactions”. The bilinear model in Lin et al. (2015) is a ‘two-stream’ architecture where distinct  
101 subnetworks model temporal and spatial aspects. The bilinear interactions are between the outputs of two  
102 CNN streams, resulting in a bilinear vector that is effectively an outer product directly on convolution  
103 maps (features are aggregated with sum-pooling). This makes intuitive sense as individual convolution  
104 maps represent specific patterns. It follows that learnable parameters representing the outer product be-  
105 tween these maps learn weightings between distinct and visualisable patterns directly. Interestingly, both  
106 Tenenbaum and Freeman (2000); Lin et al. (2015) are reminiscent of two-stream hypotheses of visual  
107 processing in the human brain Goodale and Milner (1992); Milner and Goodale (2006, 2008); Goodale  
108 (2014); Milner (2017) (discussed in detail later). Though these models focus on only visual content,  
109 their generalisable two-factor frameworks would later be inspiration to multimodal representations. Fully  
110 bilinear representations using deep learning features can easily become impractically large, necessitating  
111 informed mathematical compromises to the bilinear expansion.

### 112 **Compact Bilinear Pooling**

113 Gao et al. (2016) introduce ‘Compact Bilinear Pooling’, a technique combining the count sketch function  
114 Charikar et al. (2002) and convolution theorem Domínguez (2015) in order to ‘pool’ the outer product  
115 into a smaller bilinear representation. Fukui et al. (2016) use compact BLP in their VQA model to  
116 learn interactions between text and images i.e. multimodal compact bilinear pooling (MCB). We note  
117 that for MCB, the learned outer product is no longer on convolution maps, but rather on the indexes of  
118 image and textual tensors. Intuitively, a given index of an image or textual tensor is more abstracted  
119 from visualisable meaning when compared to convolution map. As far as we are aware, no research  
120 has addressed the potential ramifications of this switch from distinct maps to feature indexes, and later  
121 usages of bilinear pooling methods continue this trend. Though MCB is significantly more efficient  
122 than full bilinear expansions, they still require relatively large latent dimension to perform well on VQA  
123 ( $d \approx 16000$ ).

### 124 **Multimodal Low-Rank Bilinear Pooling**

125 To further reduce the number of needed parameters, Kim et al. (2017) introduce multimodal low-rank  
126 bilinear pooling (MLB), which approximates the outer product weight representation  $W$  by decomposing  
127 it into two rank-reduced projection matrices:

$$128 \quad \mathbf{z} = MLB(\mathbf{x}, \mathbf{y}) = (X^T \mathbf{x}) \odot (Y^T \mathbf{y})$$

$$129 \quad \mathbf{z} = \mathbf{x}^T W \mathbf{y} = \mathbf{x}^T X Y^T \mathbf{y} = \mathbf{1}^T (X^T \mathbf{x} \odot Y^T \mathbf{y})$$

130 where  $X \in \mathbb{R}^{m \times o}$ ,  $Y \in \mathbb{R}^{n \times o}$ ,  $o < \min(m, n)$  is the output vector dimension,  $\odot$  is element-wise multiplica-  
131 tion of vectors or the Hadamard product, and  $\mathbf{1}$  is the unity vector. MLB performs better than MCB in  
132 Osman and Samek (2019), but it is sensitive to hyperparameters and converges slowly. Furthermore, Kim  
133 et al. (2017) suggest using *Tanh* activation on the output of  $\mathbf{z}$  to further increase model capacity.

### 134 **Multimodal Factorised Low Rank Bilinear Pooling**

Yu et al. (2017) propose multimodal factorised bilinear pooling (MFB) as an extension of MLB. Consider  
the bilinear projection matrix  $W \in \mathbb{R}^{m \times n}$  outlined above, to learn output  $\mathbf{z} \in \mathbb{R}^o$  we need to learn  
 $W = [W_0, \dots, W_{o-1}]$ . We generalise output  $\mathbf{z}$ :

$$135 \quad z_i = \mathbf{x}^T \mathbf{X}_i \mathbf{Y}_i^T \mathbf{y} = \sum_{d=0}^{k-1} \mathbf{x}^T a_d b_d^T \mathbf{y} = \mathbf{1}^T (\mathbf{X}_i^T \mathbf{x} \odot \mathbf{Y}_i^T \mathbf{y}) \quad (1)$$

136 Note that MLB is equivalent to MFB where  $k=1$ . MFB can be thought of as a two-part process: features  
137 are ‘expanded’ to higher-dimensional space by  $W_\sigma$  matrices, then ‘squeezed’ into a “compact output”.  
138 The authors argue that this gives “more powerful” representational capacity in the same dimensional  
space than MLB.

### 139 **Multimodal Tucker Fusion**

140 Ben-younes et al. (2017) extend the rank-reduction concept from MLB and MFB to factorise the entire  
141 bilinear tensor using tucker decomposition Tucker (1966) in their multimodal tucker fusion (MUTAN)

142 model. We will briefly summarise the notion of rank and the mode- $n$  product to describe the tucker  
143 decomposition model.

144 **Rank and mode- $n$  product:** If  $\mathbf{W} \in \mathbb{R}^{I_1 \times \dots \times I_N}$  and  $\mathbf{V} \in \mathbb{R}^{J_n \times I_n}$  for some  $n \in \{1, \dots, N\}$  then

$$145 \quad \text{rank}(\mathbf{W} \otimes_n \mathbf{V}) \leq \text{rank}(\mathbf{W})$$

146 where  $\otimes_n$  is the mode- $n$  tensor product:

$$147 \quad (\mathbf{W} \otimes_n \mathbf{V})(i_1, \dots, i_{n-1}, j_n, i_{n+1}, \dots, i_N) := \sum_{i_n=1}^{I_n} \mathbf{W}(i_1, \dots, i_{n-1}, i_n, i_{n+1}, \dots, i_N) \mathbf{V}(j_n, i_n)$$

148 In essence, the mode- $n$  fibres (also known as mode- $n$  vectors) of  $\mathbf{W} \otimes_n \mathbf{V}$  are the mode- $n$  fibres of  $\mathbf{W}$   
149 multiplied by  $\mathbf{V}$  (proof here Guillaume OLIKIER (2017)). See Figure 1 for a visualisation of mode- $n$   
150 fibres. Each mode- $n$  tensor product introduces an upper bound to the rank of the tensor. We note that  
151 conventionally, the mode- $n$  fibres count from 1 instead of 0. We will follow this convention for the tensor  
product portion of our paper to avoid confusion. The tucker decomposition of a real  $3^{rd}$  order tensor

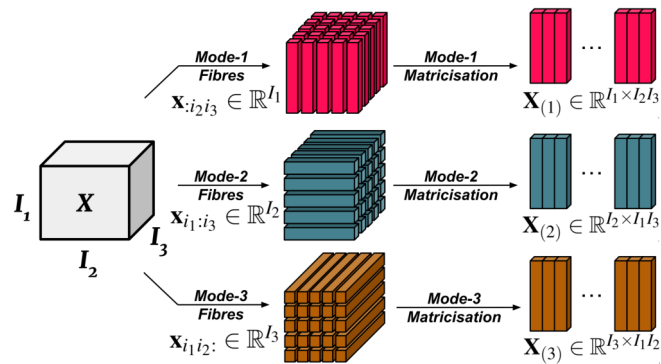


Figure 1. Visualisation of mode- $n$  fibres and matricisation

152  $\mathbf{T} \in \mathbb{R}^{d_1 \times d_2 \times d_3}$  is:

$$154 \quad \mathbf{T} = \tau \otimes_1 \mathbf{W}_1 \otimes_2 \mathbf{W}_2 \otimes_3 \mathbf{W}_3$$

155 where  $\tau \in \mathbb{R}^{d_1 \times d_2 \times d_3}$  (core tensor), and  $\mathbf{W}_1, \mathbf{W}_2, \mathbf{W}_3 \in \mathbb{R}^{d_1 \times d_1}, \mathbb{R}^{d_2 \times d_2}, \mathbb{R}^{d_3 \times d_3}$  (factor matrices) respec-  
156 tively.

157 **MUTAN:** The MUTAN model uses a reduced rank on the core tensor to constrain representational  
158 capacity, and the factor matrices to encode full bilinear projections of the textual and visual features, and  
159 finally output an answer prediction, i.e:

$$160 \quad \mathbf{y} = ((\tau \otimes_1 (\mathbf{q}^T \mathbf{W}_q)) \otimes_2 (\mathbf{v}^T \mathbf{W}_v)) \otimes_3 \mathbf{W}_o$$

161 Where  $\mathbf{y} \in \mathbb{R}^{|A|}$  is the answer prediction vector and  $\mathbf{q}, \mathbf{v}$  are the textual and visual features respectively.  
162 A slice-wise attention mechanism is used in the MUTAN model to focus on the ‘most discriminative  
163 interactions’. Multimodal tucker fusion is an empirical improvement over the preceding BLP techniques  
164 on VQA, but it introduces complex hyperparameters to refine that are important for relatively its high  
165 performance ( $\mathbf{R}$  and core tensor dimensions).

### 166 Multimodal Factorised Higher Order Bilinear Pooling

167 All the BLP techniques discussed up to now are ‘second-order’, i.e. take two functions as inputs. Yu et al.  
168 (2018b) propose multimodal factorised higher-order bilinear pooling (MFH), extending second-order  
169 BLP to ‘generalised high-order pooling’ by stacking multiple MFB units, i.e:

$$170 \quad \mathbf{z}_{exp}^i = MFB_{exp}^i(\mathbf{I}, \mathbf{Q}) = \mathbf{z}_{exp}^{i-1} \odot Dropout(\mathbf{U}^T \mathbf{I} \odot \mathbf{V}^T \mathbf{Q})$$

$$171 \quad \mathbf{z} = SumPool(\mathbf{z}_{exp})$$

172 for  $i \in \{1, \dots, p\}$  where  $\mathbf{I}, \mathbf{Q}$  are visual and text features respectively. Similar to how MFB extends MLB,  
173 MFH is MFB where  $p = 1$ . Though MFH slightly outperforms MFB, there has been little exploration  
174 into the theoretical benefit in generalising to higher-order BLP.

### 175 Bilinear Superdiagonal Fusion

176 Ben-Younes et al. (2019) proposed another method of rank restricted bilinear pooling: Bilinear Superdiag-  
 177 onal Fusion (BLOCK). We will briefly outline block term decomposition before describing BLOCK.

178 **Block Term Decomposition:** Introduced in a 3-part paper De Lathauwer (2008a,b); De Lathauwer and  
 179 Nion (2008), block term decomposition reformulates a bilinear matrix representation as the sum of rank  
 180 restricted matrix products (contrasting low rank pooling which is represented by only a single rank  
 181 restricted matrix product). By choosing the number of decompositions in the approximated sum and  
 182 their rank, block-term decompositions offer greater control over the approximated bilinear model. Block  
 183 term decompositions are easily extended to higher-order tensor decompositions, allowing multilinear  
 184 rank restriction for multilinear models in future research. A *block term decomposition* of a tensor  
 185  $\mathbf{W} \in \mathbb{R}^{I_1 \times \dots \times I_N}$  is a decomposition of the form:

$$186 \quad \mathbf{W} = \sum_{r=1}^R \mathbf{S}_r \otimes_1 \mathbf{U}_r^1 \otimes_2 \mathbf{U}_r^2 \otimes_3 \dots \otimes_n \mathbf{U}_r^n$$

187 where  $R \in \mathbb{N}^*$  and for each  $r \in \{1, \dots, R\}$ ,  $\mathbf{S}_r \in \mathbb{R}^{R_1 \times \dots \times R_n}$  where each  $\mathbf{S}_r$  are ‘core tensors’ with dimen-  
 188 sions  $R_n \leq I_n$  for  $n \in \{1, \dots, N\}$  that are used to restrict the rank of the tensor  $\mathbf{W}$ .  $\mathbf{U}_r^n \in \text{St}(R_n, I_n)$  are the  
 189 ‘factor matrices’ that intuitively expand the  $n^{\text{th}}$  dimension of  $\mathbf{S}$  back up to the original  $n^{\text{th}}$  dimension of  $\mathbf{W}$ .  
 190  $\text{St}(a, b)$  here refers to the Stiefel manifold, i.e.  $\text{St}(a, b) = \{\mathbf{Y} \in \mathbb{R}^{a \times b} : \mathbf{Y}^T \mathbf{Y} = \mathbf{I}_p\}$ . Figure 2 visualises the  
 block term decomposition process.

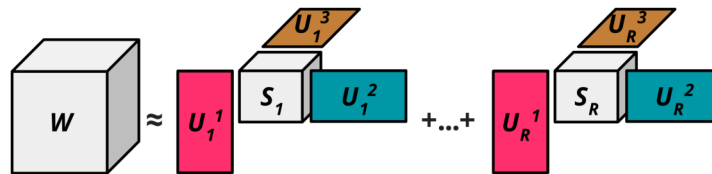


Figure 2. Block Term Decomposition (n=3)

191 **Bilinear Superdiagonal Model:** The BLOCK model uses block term decompositions to learn multimodal  
 192 interactions. The authors argue that since BLOCK enables “very rich (full bilinear) interactions between  
 193 groups of features, while the block structure limits the complexity of the whole model”, that it is able  
 194 to represent very fine grained interactions between modalities while maintaining powerful mono-modal  
 195 representations. The bilinear model with inputs  $\mathbf{x} \in \mathbb{R}^m$ ,  $\mathbf{y} \in \mathbb{R}^n$  is projected into  $o$  dimensional space with  
 196 tensor products.  
 197 tensor products:

$$198 \quad \mathbf{z} = \mathbf{W} \otimes_1 \mathbf{x} \otimes_2 \mathbf{y}$$

199 where  $\mathbf{z} \in \mathbb{R}^o$ . The superdiagonal BLOCK model uses a 3 dimensional block term decomposition. The  
 200 decomposition of  $\mathbf{W}$  in rank  $(R_1, R_2, R_3)$  is defined as:

$$201 \quad \mathbf{W} = \sum_{r=1}^R \mathbf{S}_r \otimes_1 \mathbf{U}_r^1 \otimes_2 \mathbf{U}_r^2 \otimes_3 \mathbf{U}_r^3$$

202 This can be written as

$$203 \quad \mathbf{W} = \mathbf{S}^{bd} \otimes_1 \mathbf{U}^1 \otimes_2 \mathbf{U}^2 \otimes_3 \mathbf{U}^3$$

204 where  $\mathbf{U}^1 = [\mathbf{U}_1^1, \dots, \mathbf{U}_R^1]$ , similarly with  $\mathbf{U}^2$  and  $\mathbf{U}^3$ , and now  $\mathbf{S}^{bd} \in \mathbb{R}^{RR^1 \times RR^2 \times RR^3}$ . So  $\mathbf{z}$  can now be  
 205 expressed with respect to  $\mathbf{x}$  and  $\mathbf{y}$ . Let  $\hat{\mathbf{x}} = \mathbf{U}^1 \mathbf{x} \in \mathbb{R}^{RR^1}$  and  $\hat{\mathbf{y}} = \mathbf{U}^2 \mathbf{y} \in \mathbb{R}^{RR^2}$ . These two projections are  
 206 merged by the block-superdiagonal tensor  $\mathbf{S}^{bd}$ . Each block in  $\mathbf{S}^{bd}$  merges together blocks of size  $R^1$  from  
 207  $\hat{\mathbf{x}}$  and of size  $R^2$  from  $\hat{\mathbf{y}}$  to produce a vector of size  $R^3$ :

$$208 \quad \mathbf{z}_r = \mathbf{S}_r \otimes_x \hat{\mathbf{x}}_{rR^1:(r+1)R^1} \otimes_y \hat{\mathbf{y}}_{rR^2:(r+1)R^2}$$

209 where  $\hat{\mathbf{x}}_{i:j}$  is the vector of dimension  $j - i$  containing the corresponding values of  $\hat{\mathbf{x}}$ . Finally all vectors  
 210  $\mathbf{z}_r$  are concatenated producing  $\hat{\mathbf{z}} \in \mathbb{R}^{RR^3}$ . The final prediction vector is  $\mathbf{z} = \mathbf{U}^3 \hat{\mathbf{z}} \in \mathbb{R}^o$ . Similar to tucker  
 211 fusion, the block term decomposition based fusion in BLOCK theoretically allows more nuanced control  
 212 on representation size and empirically outperforms previous techniques.

## 213 RELATED WORKS

### 214 Bilinear Pooling in Video-QA With Language-Vision Fusion

215 We aim to highlight and explore a broad shift away from BLP in favour of methods such as attention  
216 in video-QA benchmarks. Several video models have incorporated and contrasted BLP techniques to  
217 their own model designs for language-vision fusion tasks. Kim et al. (2019) find various BLP fusions  
218 perform worse than their ‘dynamic modality fusion’ mechanism on TVQA Lei et al. (2018) and MovieQA  
219 Tapaswi et al. (2016). Li et al. (2019) find MCB fusion performs worse on their model in ablation  
220 studies on TGIF-QA Jang et al. (2017). Chou et al. (2020) use MLB as part of their baseline model  
221 proposed alongside their ‘VQA 360°’ dataset. Gao et al. (2019) contrast their proposed two-stream  
222 attention mechanism to an MCB model for TGIF-QA, demonstrating a substantial performance increase  
223 over the MCB model. Liu et al. (2021) use MUTAN fusion between question and visual features to  
224 yield impressive results on TGif-QA, though they are outperformed by an attention based model using  
225 element-wise multiplication Le et al. (2020). The Focal Visual-Text Attention network (FVTA) Liang  
226 et al. (2019) is a hierarchical model that aims to dynamically select from the appropriate point across both  
227 time and modalities that outperforms an MCB approach on Movie-QA.

### 228 Bilinear Pooling in Video Without Language-Vision Fusion

229 Where recent research in video-QA tasks (which includes textual questions as input) has moved away  
230 from BLP techniques, several video tasks that do *not* involve language have found success using BLP  
231 techniques. Zhou et al. (2021) use a multilevel factorised BLP based model to fuse audio and visual  
232 features for emotion recognition in videos. Hu et al. (2021) use compact BLP to fuse audio and ‘visual  
233 long range’ features for human action recognition. Pang et al. (2021) use MLB as part of an attention-  
234 based fusion for audio and visual features for violence detection in videos. Xu et al. (2021) use BLP to  
235 fuse visual features from different channels in RGBT tracking. Deng et al. (2021) use compact BLP to  
236 fuse spatial and temporal representations of video features for action recognition. Wang et al. (2021)  
237 fuse motion and appearance visual information together achieving state-of-the-art results on MSVD-QA.  
238 Sudhakaran et al. (2021) draw design inspiration from bilinear processing of Lin et al. (2015) and MCB  
239 to propose ‘Class Activation Pooling’ for video action recognition. Deb et al. (2022) use MLB to process  
240 video features for video captioning.

## 241 DATASETS

242 In this section, we outline the video-QA datasets we use in our experiments.

### 243 MSVD-QA

244 Xu et al. (2017) argue that simply extending image-QA methods is “insufficient and suboptimal” to  
245 conduce quality video-QA, and that instead the focus should be on the temporal structure of videos. Using  
246 an NLP method to automatically generate QA pairs from descriptions Heilman and Smith (2009), Xu  
247 et al. (2017) create the MSVD-QA dataset based on the Microsoft research video description corpus Chen  
248 and Dolan (2011). The dataset is made from 1970 video clips, with over 50k QA pairs in ‘5w’ style i.e.  
249 (“what”, “who”, “how”, “when”, “where”).

### 250 TGIF-QA

251 Jang et al. (2017) speculate that the relatively limited progress in video-QA compared to image-QA is  
252 “due in part to the lack of large-scale datasets with well defined tasks”. As such, they introduced the  
253 TGIF-QA dataset to ‘complement rather than compete’ with existing VQA literature and to serve as a  
254 bridge between video-QA and video understanding. To this end, they propose 3 subsets with specific  
255 video-QA tasks that aim to take advantage of the temporal format of videos:

256 **Count:** Counting the number of times a specific action is repeated Levy and Wolf (2015) e.g. “How many  
257 times does the girl jump?”. Models output the predicted number of times the specified actions happened.  
258 (Over 30k QA pairs).

259 **Action:** Identify the action that is repeated a number of times in the video clip. There are over 22k  
260 multiple choice questions e.g. “What does the girl do 5 times?”.

261 **Trans:** Identifying details about a state transition Isola et al. (2015). There are over 58k multiple choice  
262 questions e.g. “What does the man do after the goal post?”.

263 **Frame-QA:** An image-QA split using automatically generated QA pairs from frames and captions in the  
264 TGIF dataset Li et al. (2016) (over 53k multiple choice questions).

### 265 TVQA

266 The TVQA dataset Lei et al. (2018) is designed to address the shortcomings of previous datasets. It  
267 has significantly longer clip lengths than other datasets and is based on TV shows instead of cartoons  
268 to give it realistic video content with simple coherent narratives. It contains over 150k QA pairs. Each  
269 question is labelled with timestamps for the relevant video frames and subtitles. The questions were  
270 gathered using AMT workers. Most notably, the questions were specifically designed to encourage  
271 multimodal reasoning by asking the workers to design two-part compositional questions. The first part  
272 asks a question about a ‘moment’ and the second part localises the relevant moment in the video clip i.e.  
273 [What/How/Where/Why/Who/...] — [when/before/after] —, e.g. ‘[What] was House saying [before] he  
274 leaned over the bed?’. The authors argue this facilitates questions that require both visual and language  
275 information since “people often naturally use visual signals to ground questions in time”. The authors  
276 identify certain biases in the dataset. They find that the average length of correct answers are longer  
277 than incorrect answers. They analyse the performance of their proposed baseline model with different  
278 combinations of visual and textual features on different question types they have identified. Though recent  
279 analysis has highlighted bias towards subtitles in TVQA’s questions Winterbottom et al. (2020), it remains  
280 an important large scale video-QA benchmark.

### 281 EgoVQA

282 Most video-QA datasets focus on video-clips from the 3<sup>rd</sup> person. Fan (2019) argue that 1<sup>st</sup> person  
283 video-QA has more natural use cases that real-world agents would need. As such, they propose the  
284 egocentric video-QA dataset (EgoVQA) with 609 QA pairs on 16 first-person video clips. Though the  
285 dataset is relatively small, it has a diverse set of question types (e.g. 1<sup>st</sup> & 3<sup>rd</sup> person ‘action’ and ‘who’  
286 questions, ‘count’, ‘colour’ etc.), and aims to generate hard and confusing incorrect answers by sampling  
287 from correct answers of the same question type. Models on EgoVQA have been shown to overfit due to its  
288 small size. To remedy this, Fan (2019) pretrain the baseline models on the larger YouTube2Text-QA Ye  
289 et al. (2017). YouTube2Text-QA is a multiple choice dataset created from MSVD videos Chen and Dolan  
290 (2011) and questions created from YouTube2Text video description corpus Guadarrama et al. (2013).  
291 YouTube2Text-QA has over 99k questions in ‘what’, ‘who’ and ‘other’ style.

## 292 MODELS

293 In this section, we describe the models used in our experiments, built from the official TVQA <sup>1</sup> and  
294 HME-VideoQA <sup>2</sup> implementations.

### 295 TVQA Model

296 **Model Definition:** The model takes as inputs: a question  $q$ , five potential answers  $\{a_i\}_{i=0}^4$ , a subtitle  $S$   
297 and corresponding video-clip  $V$ , and outputs the predicted answer. As the model can either use the entire  
298 video-clip and subtitle or only the parts specified in the timestamp, we refer to the sections of video and  
299 subtitle used as segments from now on. Figure 3 demonstrates the textual and visual streams and their  
300 associated features in model architecture.

301 **ImageNet Features:** Each frame is processed by a ResNet101 He et al. (2016) pretrained on ImageNet  
302 Deng et al. (2009) to produce a 2048-d vector. These vectors are then L2-normalised and stacked in frame  
303 order:  $V^{img} \in \mathbb{R}^{f \times 2048}$  where  $f$  is the number of frames used in the video segment.

304 **Regional Features:** Each frame is processed by a Faster R-CNN Ren et al. (2015) trained on Visual  
305 Genome Krishna et al. (2017) in order to detect objects. Each detected object in the frame is given a  
306 bounding box, and has an affiliated 2048-d feature extracted. Since there are multiple objects detected per  
307 frame (we cap it at 20 per frame), it is difficult to efficiently represent this in time sequences Lei et al.  
308 (2018). The model uses the top-K regions for all detected labels in the segment as in Anderson et al.  
309 (2018) and Karpathy and Fei-Fei (2015). Hence the regional features are  $V^{reg} \in \mathbb{R}^{n_{reg} \times 2048}$  where  $n_{reg}$   
310 is the number of regional features used in the segment.

<sup>1</sup><https://github.com/jayleicn/TVQA>

<sup>2</sup><https://github.com/fanchenyou/HME-VideoQA>

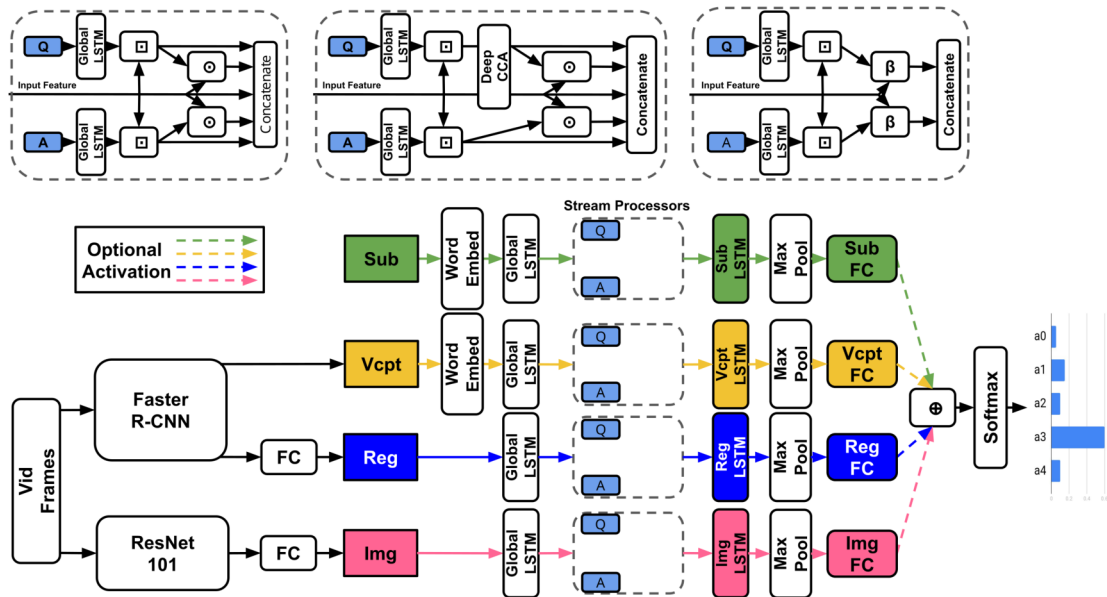


**Figure 3.** TVQA Model.  $\odot/\oplus$  = Element-wise multiplication/addition,  $\square$  = context matching Seo et al. (2017); Yu et al. (2018a),  $\beta$  = BLP. Any feature streams may be enabled/disabled.

311 **Visual Concepts:** The classes or labels of the detected regional features are called ‘Visual Concepts’. Yin  
 312 and Ordonez (2017) found that simply using detected labels instead of image features gives comparable  
 313 performance on image captioning tasks. Importantly they argued that combining CNN features with  
 314 detected labels outperforms either approach alone. Visual concepts are represented as either GloVe  
 315 Pennington et al. (2014) or BERT Devlin et al. (2019) embeddings  $V^{vcpt} \in \mathbb{R}^{n_{vcpt} \times 300}$  or  $\mathbb{R}^{n_{vcpt} \times 768}$   
 316 respectively, where  $n_{vcpt}$  is the number of visual concepts used in the segment.

317 **Text Features:** The model encodes the questions, answers, and subtitles using either GloVe ( $\in \mathbb{R}^{300}$ ) or  
 318 BERT embeddings ( $\in \mathbb{R}^{768}$ ). Formally,  $q \in \mathbb{R}^{n_q \times d}$ ,  $\{a_i\}_{i=0}^4 \in \mathbb{R}^{n_{a_i} \times d}$ ,  $S \in \mathbb{R}^{n_s \times d}$  where  $n_q, n_{a_i}, n_s$  is  
 319 the number of words in  $q, a_i, S$  respectively and  $d = 300, 768$  for GloVe or BERT embeddings respectively.

320 **Context Matching:** Context matching refers to context-query attention layers recently adopted in machine  
 321 comprehension Seo et al. (2017); Yu et al. (2018a). Given a context-query pair, context matching layers  
 322 return ‘context aware queries’.

323 **Model Details:** Any combination of subtitles or visual features can be used. All features are mapped into  
 324 word vector space through a tanh non-linear layer. They are then processed by a shared bi-directional  
 325 LSTM Hochreiter and Schmidhuber (1997); Graves and Schmidhuber (2005) (‘Global LSTM’ in Figure  
 326 3) of output dimension 300. Features are context-matched with the question and answers. The original  
 327 context vector is then concatenated with the context-aware question and answer representations and  
 328 their combined element-wise product (‘Stream Processor’ in Figure 3, e.g. for subtitles  $S$ , the stream  
 329 processor outputs  $[F^{sub}, A^{sub,q}, A^{sub,a_0-4}, F^{sub} \odot A^{sub,q}, F^{sub} \odot A^{sub,a_0-4}] \in \mathbb{R}^{n_{sub} \times 1500}$  where  $F^{sub} \in \mathbb{R}^{n_s \times 300}$ .  
 330 Each concatenated vector is processed by their own unique bi-directional LSTM of output dimension 600,  
 331 followed by a pair of fully connected layers of output dimensions 500 and 5, both with dropout 0.5 and  
 332 ReLU activation. The 5-dimensional output represents a vote for each answer. The element-wise sum  
 333 of each activated feature stream is passed to a softmax producing the predicted answer ID. All features  
 334 remain separate through the entire network, effectively allowing the model to choose the most useful  
 335 features.

### 336 HME-VideoQA

337 To better handle semantic meaning through long sequential video data, recent models have integrated  
 338 external ‘memory’ units Xiong et al. (2016); Sukhbaatar et al. (2015) alongside recurrent networks to  
 339 handle input features Gao et al. (2018); Zeng et al. (2017). These external memory units are designed  
 340 to encourage multiple iterations of inference between questions and video features, helping the model  
 341 revise it’s visual understanding as new details from the question are presented. The heterogeneous

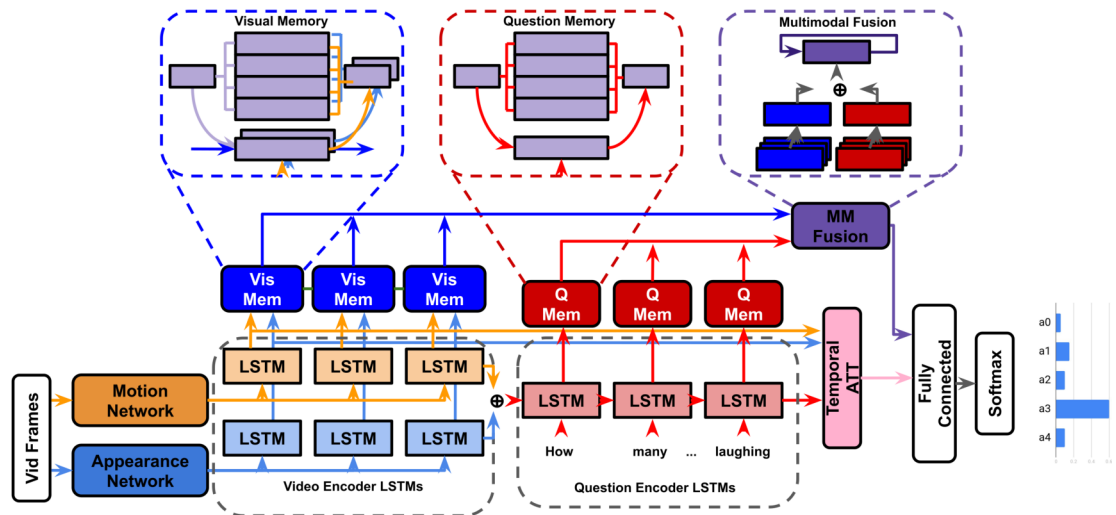


Figure 4. HME Model

342 memory-enhanced video-QA model (HME) Fan et al. (2019) proposes several improvements to previous  
 343 memory based architectures:

344 **Heterogeneous Read/Write Memory:** The memory units in HME use an attention-guided read/write  
 345 mechanism to read from/update memory units respectively (the number of memory slots used is a hyper-  
 346 parameter). The claim is that since motion and appearance features are heterogeneous, a ‘straightforward’  
 347 combination of them cannot effectively describe visual information. The video memory aims to effectively  
 348 fuse motion (C3D Tran et al. (2014)) and appearance (ResNet He et al. (2016) and VGG Simonyan  
 349 and Zisserman (2015)) features by integrating them in the joint read/write operations (visual memory in  
 350 Figure 4).

351 **Encoder-Aware Question Memory:** Previous memory models used a single feature vector outputted  
 352 by an LSTM or GRU for their question representation Gao et al. (2018); Zeng et al. (2017); Xiong et al.  
 353 (2016); Anderson et al. (2018). HME uses an LSTM question encoder and question memory unit pair that  
 354 augment each other dynamically (question memory in Figure 4).

355 **Multimodal Fusion Unit:** The hidden states of the video and question memory units are processed by a  
 356 temporal attention mechanism. The joint representation ‘read’ updates the fusion unit’s own hidden state.  
 357 The visual and question representations are ultimately fused by vector concatenation (multimodal fusion  
 in Figure 5). Our experiments will involve replacing this concatenation step with BLP techniques.

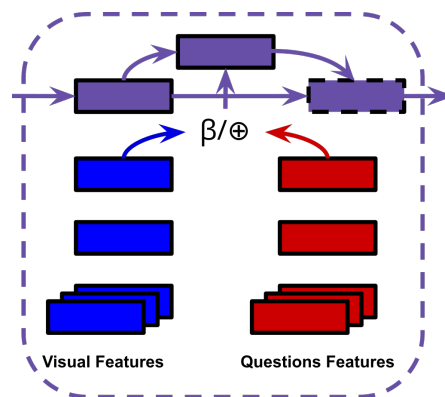


Figure 5.  $\oplus$  = Concatenation,  $\beta$  = BLP.

358

## 359 EXPERIMENTS AND RESULTS

360 In this section we outline our experimental setup and results. We save our insights for the discussion  
 361 in the next section. See our GitHub repository<sup>3</sup> for both the datasets and code used in our experiments.  
 Table 1 shows the benchmarks and SotA results for the datasets we consider in this paper.

Dataset	Benchmark	SoTA
TVQA (Val)	68.85% Lei et al. (2018)	74.97% Khan et al. (2020)
TVQA (Test)	68.48% Lei et al. (2018)	72.89% Khan et al. (2020)
EgoVQA (Val 1)	37.57% Fan (2019)	45.05%* Chenyou (2019)
EgoVQA (Test 2)	31.02% Fan (2019)	43.35%* Chenyou (2019)
MSVD-QA	32.00% Xu et al. (2017)	40.30% Guo et al. (2021)
TGIF-Action	60.77% Jang et al. (2017)	84.70% Le et al. (2020)
TGIF-Count	4.28† Jang et al. (2017)	2.19† Le et al. (2020)
TGIF-Trans	67.06% Jang et al. (2017)	87.40% Seo et al. (2021)
TGIF-FrameQA	49.27% Jang et al. (2017)	64.80% Le et al. (2020)

**Table 1.** Dataset benchmark and SoTA results to the best of our knowledge. † = Mean L2 loss. \* = Results we replicated using the cited implementation.

362

### 363 Concatenation to BLP (TVQA)

364 As previously discussed, BLP techniques have outperformed feature concatenation on a number of VQA  
 365 benchmarks. The baseline stream processor concatenates the visual feature vector with question and  
 366 answer representations. Each of the 5 inputs to the final concatenation are 300-d. We replace the visual-  
 367 question/answer concatenation with BLP (Figure 6). All inputs to the BLP layer are 300-d, the outputs  
 368 are 750-d and the hidden size is 1600 (a smaller hidden state than normal, however, the input features are  
 369 also smaller compared to other uses of BLP). We make as few changes as possible to accommodate BLP,  
 370 i.e. we use context matching to facilitate BLP fusion by aligning visual and textual features temporally.  
 Our experiments include models with/without subtitles or questions (Table 2).

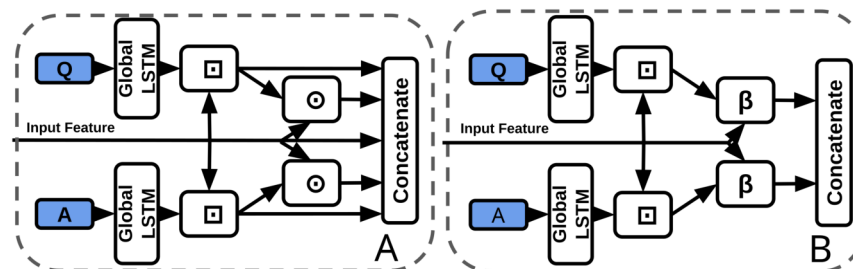


**Figure 6.** Baseline concatenation stream processor from TVQA model (left-A) vs Our BLP stream processor (right-B).  $\odot$  = Element-wise multiplication,  $\beta$  = BLP,  $\square$  = Context Matching.

371

### 372 Dual-Stream Model

373 We create our ‘dual-stream’ (Figure 7, Table 3) model from the SI TVQA baseline model for 2 main  
 374 purposes: **I)** To explore the effects of a joint representation on TVQA, **II)** To contrast the concatenation-  
 375 replacement experiment with a model restructured specifically with BLP as a focus. The baseline BLP  
 376 model keeps subtitles and other visual features completely separate up to the answer voting step. Our aim  
 377 here is to create a joint representation BLP-based model similar in essence to the baseline TVQA model  
 378 that fuses subtitle and visual features. As before, we use context matching to temporally align the video  
 379 and text features.

<sup>3</sup>[https://github.com/Jumperkables/trying\\_blp](https://github.com/Jumperkables/trying_blp)

Subtitles	Fusion Type	Accuracy	Baseline Offset
-	Concatenation	45.94%	-
GloVE	Concatenation	69.74%	-
BERT	Concatenation	72.20%	-
- (No Q)	Concatenation	45.58%	-0.36%
GloVE (No Q)	Concatenation	68.31%	-1.42%
BERT (No Q)	Concatenation	70.43%	-1.77%
-	MCB	<b>45.65%</b>	<b>-0.29%</b>
GloVE	MCB	<b>69.32%</b>	<b>-0.42%</b>
BERT	MCB	<b>71.68%</b>	<b>-0.52%</b>
-	MLB	41.98%	-3.96%
GloVE	MLB	69.30%	-0.44%
BERT	MLB	69.04%	-3.16%
-	MFB	41.82%	-4.12%
GloVE	MFB	68.87%	-0.87%
BERT	MFB	67.29%	-4.91%
-	MFH	44.44%	-1.5%
GloVE	MFH	68.43%	-1.31%
BERT	MFH	67.29%	-4.91%
-	Blocktucker	44.44%	-1.5%
GloVE	Blocktucker	67.95%	-1.79%
BERT	Blocktucker	67.04%	-5.16%
-	BLOCK	41.09%	-4.85%
GloVE	BLOCK	65.31%	-4.43%
BERT	BLOCK	66.94%	-5.26%

**Table 2.** Concatenation replaced with BLP in the TVQA model on the TVQA Dataset. All models use visual concepts and ImageNet features. ‘No Q’ indicates questions are not used as inputs i.e. answers rely purely on input features.

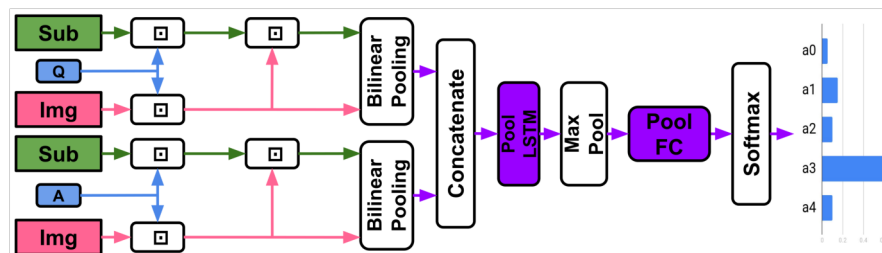


**Figure 7.** Our Dual-Stream Model.  $\square$  = Context Matching.

### 380 Deep CCA in TVQA

381 In contrast to joint representations, Baltrušaitis et al. (2019) define ‘co-ordinated representations’ as a  
 382 category of multimodal fusion techniques that learn “separated but co-ordinated” representations for  
 383 each modality (under some constraints). Peng et al. (2018) claim that since there is often an information  
 384 imbalance between modalities, learning separate modality representations can be beneficial for preserving  
 385 ‘exclusive and useful modality-specific characteristics’. We include one such representation, deep canonical  
 386 correlation analysis (DCCA) Andrew et al. (2013), in our experiments to contrast with the joint BLP  
 387 models.

### 388 CCA

389 Canonical cross correlation analysis (CCA) Hotelling (1936) is a method for measuring the correlations  
 390 between two sets. Let  $(\mathbf{X}_0, \mathbf{X}_1) \in \mathbb{R}^{d_0} \times \mathbb{R}^{d_1}$  be random vectors with covariances  $(\Sigma_{r=00}, \Sigma_{r=11})$  and  
 391 cross-covariance  $\Sigma_{r=01}$ . CCA finds pairs of linear projections of the two views  $(w'_0 \mathbf{X}_0, w'_1 \mathbf{X}_1)$  that are  
 392 maximally correlated:

$$393 \rho = (w_0^*, w_1^*) = \underset{w_0, w_1}{\operatorname{argmax}} \operatorname{corr}(w'_0 \mathbf{X}_0, w'_1 \mathbf{X}_1)$$

$$= \underset{w_0, w_1}{\operatorname{argmax}} \frac{w'_0 \Sigma_{01} w_1}{\sqrt{w'_0 \Sigma_{00} w_0 w'_1 \Sigma_{11} w_1}}$$

where  $\rho$  is the correlation co-efficient. As  $\rho$  is invariant to the scaling of  $w_0$  and  $w_1$ , the projections are constrained to have unit variances, and can be represented as the following maximisation:

$$\underset{w_0, w_1}{\operatorname{argmax}} w'_0 \Sigma_{01} w_1 \text{ s.t. } w'_0 \Sigma_{00} w_0 = w'_1 \Sigma_{11} w_1 = \mathbf{1}$$

However, CCA can only model linear relationships regardless of the underlying realities in the dataset. Thus, CCA extensions were proposed, including kernel CCA (KCCA) Akaho (2001) and later DCCA.

#### DCCA

DCCA is a parametric method used in multimodal neural networks that can learn non-linear transformations for input modalities. Both modalities  $t, v$  are encoded in neural-network transformations  $H_t, H_v = f_t(t, \theta_t), f_v(v, \theta_v)$ , and then the canonical correlation between both modalities is maximised in a common subspace (i.e. maximise cross-modal correlation between  $H_t, H_v$ ).

$$\max_{\theta_t, \theta_v} \operatorname{corr}(H_t, H_v) = \underset{\theta_t, \theta_v}{\operatorname{argmax}} \operatorname{corr}(f_t(t, \theta_t), f_v(v, \theta_v))$$

We use DCCA over KCCA to co-ordinate modalities in our experiments as it is generally more stable and efficient, learning more ‘general’ functions.

#### DCCA in TVQA

We use a 2-layer DCCA module to coordinate question and context (visual or subtitle) features (Figure 8, Table 4). Output features are the same dimensions as inputs. Though DCCA itself is not directly related to BLP, it has recently been classified as a coordinated representation Guo et al. (2019), which contrasts a ‘joint’ representation.

Model	Text	Val Acc
TVQA SI	GloVe	67.78%
TVQA SI	BERT	70.56%
Dual-Stream MCB	GloVe	63.46%
Dual-Stream MCB	BERT	60.63%
Dual-Stream MFH	GloVe	62.71%
Dual-Stream MFH	BERT	59.34%

**Table 3.** Dual-Stream Results Table. ‘SI’ for TVQA models indicates the model is using subtitle and ImageNet feature streams only, i.e. the green and pink streams in Figure 3

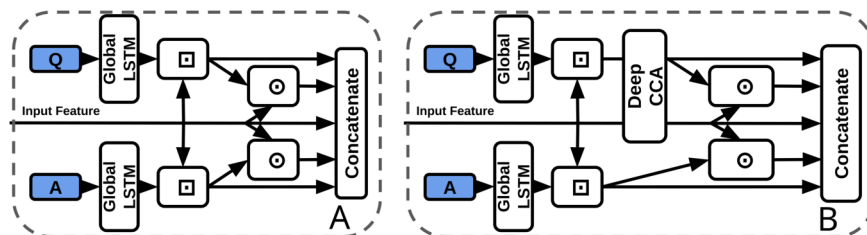


**Figure 8.** Baseline concatenation stream processor from TVQA model (left-A) vs Our DCCA stream processor (right-B).  $\odot$  = Element-wise multiplication,  $\square$  = Context Matching.

#### Concatenation to BLP (HME-VideoQA)

As described in the previous section, we replace a concatenation step in the HME model between textual and visual features with BLP (Figure 5, corresponding to the multimodal fusion unit in Figure 4). The goal here is to explore if BLP can better facilitate multimodal fusion in aggregated memory features (Table 5). We replicate the results from Fan et al. (2019) with the HME on the MSVD, TGIF and EgoVQA datasets using the official github repository Chenyou (2019). We extract our own C3D features from the frames in the TVQA.

Model	Text	Baseline Acc	DCCA Acc
VI	GloVe	45.94%	45.00% (-0.94%)
VI	BERT	–	41.70%
SVI	GloVe	69.74%	67.91% (-1.83%)
SVI	BERT	72.20%	68.48% (-3.72%)

**Table 4.** DCCA in the TVQA Baseline Model.

Dataset	Fusion Type	Val	Test
TVQA (GloVe)	Concatenation	41.25%	N/A
EgoVQA-0	Concatenation	36.99%	37.12%
EgoVQA-1	Concatenation	48.50%	43.35%
EgoVQA-2	Concatenation	45.05%	39.04%
MSVD-QA	Concatenation	30.94%	33.42%
TGIF-Action	Concatenation	70.69%	73.87%
TGIF-Count	Concatenation	3.95†	3.92†
TGIF-Trans	Concatenation	76.33%	78.94%
TGIF-FrameQA	Concatenation	52.48%	51.41%
TVQA (GloVe)	MCB	41.09% (-0.16%)	N/A%
EgoVQA-0	MCB	No Convergence	No Convergence
EgoVQA-1	MCB	No Convergence	No Convergence
EgoVQA-2	MCB	No Convergence	No Convergence
MSVD-QA	MCB	30.85% (-0.09%)	33.78% (+0.36%)
TGIF-Action	MCB	73.56% (+2.87%)	73.00% (-0.87%)
TGIF-Count	MCB	3.95† (+0†)	3.98† (+0.06†)
TGIF-Trans	MCB	79.30% (+2.97%)	77.10% (-1.84%)
TGIF-FrameQA	MCB	51.72% (-0.76%)	52.21% (+0.80%)

**Table 5.** HME-VideoQA Model. The default fusion technique is concatenation. † refers to minimised L2 loss.

## DISCUSSION

### TVQA Experiments

**No BLP Improvements on TVQA:** On the HME concat-to-BLP substitution model (Table 5), MCB barely changes model performance at all. We find that none of our TVQA concat-to-BLP substitutions (Table 2) yield any improvements at all, with almost all of them performing worse overall (0.3-5%) than even the questionless concatenation model. Curiously, MCB scores the highest of all BLP techniques. The dual-stream model performs worse still, dropping accuracy by between 5-10% vs the baseline (Table 3). Similarly, we find that MCB performs best despite being known to require larger latent spaces to work on VQA.

**BERT Impacted the Most:** For the TVQA BLP-substitution models, we find the GloVe, BERT and ‘no-subtitle’ variations all degrade by roughly similar margins, with BERT models degrading more most often. This slight discrepancy is unsurprising as the most stable BERT baseline model is the best, and thus may degrade more on the inferior BLP variations. However, BERT’s relative degradation is much more pronounced on the dual-stream models, performing 3% worse than GloVe. We theorise that here, the significant and consistent drop is potentially caused by BERT’s more contextual nature is no longer helping, but actively obscuring more pronounced semantic meaning learned from subtitles and questions.

**Blame Smaller Latent Spaces?:** Naturally, bilinear representations of time series data across multiple frames or subtitles are highly VRAM intensive. Thus we can only explore relatively small hidden dimensions (i.e. 1600). However, we cannot simply conclude our poor results are due to our relatively small latent spaces because: **I**) MCB is our best performing BLP technique. However, MCB has been outperformed by MFH on previous VQA models *and* it has been shown to require much larger latent spaces to work effectively in the first place Fukui et al. (2016) (16000). **II**) Our vector representations of text and images are also much smaller (300-d) compared to the larger representation dimensions conventional in previous benchmarks (e.g. 2048 in Fukui et al. (2016)). We note that  $16000/2048 \approx 1600/300$ , and so our latent-to-input size ratio is not substantially different to previous works.

445 **Unimodal Biases in TVQA and Joint Representation:** Another explanation may come from works  
446 exploring textual biases inherent in TVQA to textual modalities Winterbottom et al. (2020). BLP has been  
447 categorised as a ‘joint representation’. Baltrušaitis et al. (2019) consider representation as summarising  
448 multimodal data “in a way that exploits the complementarity and redundancy of multiple modalities”.  
449 Joint representations combine unimodal signals into the same representation space. However, they struggle  
450 to handle missing data Baltrušaitis et al. (2019) as they tend to preserve shared semantics while ignoring  
451 modality-specific information Guo et al. (2019). The existence of unimodal text bias in TVQA implies  
452 BLP may perform poorly on the TVQA as a joint representation of it’s features because: **I)** information  
453 from either modality is consistently missing, **II)** prioritising ‘shared semantics’ over ‘modality-specific’  
454 information harms performance on TVQA. Though concatenation could also be classified as a joint  
455 representation, we argue that this observation still has merit. Theoretically, a concatenation layer can still  
456 model modality specific information (see Figure 9), but a bilinear representation would seem to inherently  
457 entangle its inputs which would make modality specific information more challenging to learn since each  
458 parameter representing one modality is by definition weighted with the other. This may explain why our  
459 simpler BLP substitutions perform better than our more drastic ‘joint’ dual-stream model.

460 **What About DCCA?:** Table 4 shows our results on the DCCA augmented TVQA models. We see a  
461 slight but noticable performance degradation with this relatively minor alteration to the stream processor.  
462 As previously mentioned, DCCA is in some respects an opposite approach to multimodal fusion than  
463 BLP, i.e. a ‘coordinated representation’. The idea of a coordinated representations is to learn a separate  
464 representation for each modality , but with respect to the other. In this way, it is thought that multimodal  
465 interactions can be learned while still preserving modality-specific information that a joint representation  
466 may otherwise overlook Guo et al. (2019); Peng et al. (2018). DCCA specifically maximises cross-modal  
467 correlation. Without further insight from surrounding literature, it is difficult to conclude what TVQA’s  
468 drop in performance using both joint *and* coordinated representations could mean. We will revisit this  
469 when we discuss the role of attention in multimodal fusion.

470 **Does Context Matching Ruin Multimodal Integrity?:** The context matching technique used in the  
471 TVQA model is the bidirectional attention flow (BiDAF) module introduced in Seo et al. (2017). It is  
472 used in machine comprehension between a textual context-query pair to generate query-aware context  
473 representations. BiDAF uses a ‘memoryless’ attention mechanism where information from each time  
474 step does not directly affect the next, which is thought to prevent early summarisation. BiDAF considers  
475 different input features at different levels of granularity. The TVQA model uses bidirectional attention  
476 flow to create context aware (visual/subtitle) question and answer representations. BiDAF can be seen as  
477 a co-ordinated representation in some regards, but it does project questions and answers representations  
478 into a new space. We use this technique to prepare our visual and question/answer features because it  
479 temporally aligns both features, giving them the same dimensional shape, conveniently allowing us to  
480 apply BLP at each time step. Since the representations generated are much more similar than the original  
481 raw features and there is some degree of information exchange, it may affect BLP’s representational  
482 capacity. Though it is worth considering these potential shortcomings, we cannot immediately assume  
483 that BiDAF would cause serious issues as earlier bilinear technique were successfully used between  
484 representations in the same modality Tenenbaum and Freeman (2000); Gao et al. (2016). This implies that  
485 multimodal interactions can still be learned between the more similar context-matched representations,  
486 provided the information is still present. Since BiDAF does allow visual information to be used in the  
487 TVQA baseline model, it is reasonable to assume that some of the visual information is in fact intact and  
488 exploitable for BLP. However, it is still currently unclear if context matching is fundamentally disrupting  
489 BLP and contributing to the poor results we find. We note that in BiDAF, ‘memoryless’ attention is  
490 implemented to avoid propagating errors through time. We argue that though this may be true and help in  
491 some circumstances, conversely, this will not allow some useful interactions to build up over time steps.

## 492 **The Other Datasets on HME**

493 **BLP Has No Effect:** Our experiments on the EgoVQA, TGIF-QA and MSVD-QA datasets are on  
494 concat-to-BLP substitution HME models. Our results are inconclusive. There is virtually no variation in  
495 performance between the BLP and concatenation implementations. Interestingly, EgoVQA consistently  
496 does not converge with this simple substitution. We cannot comment for certain on why this is the case.  
497 There seems to be no intuitive reason why it’s 1<sup>st</sup> person content would cause this. Rather, we believe this  
498 is symptomatic of overfitting in training, as EgoVQA is very small *and* pretrained on a different dataset,

499 and BLP techniques can sometimes have difficulties converging.

500 **Does Better Attention Explain the Difference?:** Attention mechanisms have been shown to improve  
501 the quality of text and visual interactions. Yu et al. (2017) argue that methods without attention are  
502 ‘coarse joint-embedding models’ which use global features that contain noisy information unhelpful in  
503 answering fine-grained questions commonly seen in VQA and video-QA. This provides strong motivation  
504 for implementing attention mechanisms alongside BLP, so that the theoretically greater representational  
505 capacity of BLP is not squandered on less useful noisy information. The TVQA model uses the previously  
506 discussed BiDAF mechanism to focus information from both modalities. However, the HME model  
507 integrates a more complex memory-based multi-hop attention mechanism. This difference may potentially  
508 highlight why the TVQA model suffers more substantially integrating BLP than the HME one.

### 509 **BLP in Video-QA: Problems and Recommendations**

510 We have experimented with BLP in 2 video-QA models and across 4 datasets. Our experiments show  
511 that the BLP fusion techniques popularised in VQA has not extended to increased performance to video-  
512 QA. In the preceding sections, we have supported this observation with experimental results which we  
513 contextualise by surveying the surrounding literature for BLP for multimodal video tasks. In this section,  
514 we condense our observations into a list of problems that BLP techniques pose to video-QA, and our  
515 proposal for alternatives and solutions:

516 **Inefficient and Computationally Expensive Across Time:** BLP as a fusion mechanism in video-QA  
517 can be exceedingly expensive due to added temporal relations. Though propagating information from  
518 each time step through a complex text-vision multimodal fusion layer is an attractive prospect, our  
519 experiments imply that modern BLP techniques simply do not empirically perform in such a scenario.  
520 We recommend avoiding computationally expensive fusion techniques like BLP for text-image fusion  
521 *throughout* timesteps, and instead simply concatenate features at these points to save computational  
522 resources for other stages of processing (e.g. attention). Furthermore, we note that any prospective fusion  
523 technique used across time will quickly encounter memory limitations that could force the hidden-size  
524 used sub-optimally low. Though summarising across time steps into condensed representations may  
525 allow more expensive BLP layers to be used on the resultant text and video representations, we instead  
526 recommend using state-of-the-art and empirically proven multimodal attention mechanisms instead Lei  
527 et al. (2021); Yang et al. (2021). Attention mechanisms are pivotal in VQA for reducing noise and focusing  
528 on specific fine-grained details Yu et al. (2017). The sheer increase in feature information when moving  
529 from still-image to video further increases the importance of attention in video-QA. Our experiments  
530 show the temporal-attention based HME model performs better when it is not degraded by BLP. Our  
531 findings are in line with that of Long et al. (2018) as they consider multiple different fusion methods  
532 for video classification, i.e. LSTM, probability, ‘feature’ and attention. ‘Feature’ fusion is the direct  
533 connection of each modality within each local time interval, which is effectively what context matching  
534 does in the TVQA model. Long et al. (2018) finds temporal feature based fusion sub-par, and speculates  
535 that the burden of learning multimodal *and* temporal interactions is too heavy. Our experiments lend  
536 further evidence that for video tasks, attention-based fusion is the ideal choice.

537 **Problem with Alignment of Text and Video:** As we highlight in the second subsection of our related  
538 works, BLP has yielded great performance in video tasks where it fuses the visual features with *non-textual*  
539 features. Audio and visual feature fusion demonstrates impressive performance on action recognition Hu  
540 et al. (2021), emotion recognition Zhou et al. (2021), and violence detection Pang et al. (2021). Likewise,  
541 different visual representations have thrived in RGBT tracking Xu et al. (2021), action recognition Deng  
542 et al. (2021) and video-QA on MSVD-QA Wang et al. (2021). On the other hand, we notice that several  
543 recent video-QA works (highlighted in the first section of our related works) have found in ablation  
544 that BLP fusion which specifically fuse visual and *textual* features give poor results Kim et al. (2019);  
545 Li et al. (2019); Gao et al. (2019); Liu et al. (2021); Liang et al. (2019). Our observations and our  
546 experimental results highlight a pattern of poor performance for BLP in text-video fusion specifically.  
547 We demonstrate poor performance using BLP to fuse both ‘BiDAF-aligned’ (TVQA) and ‘raw’ (HME)  
548 text and video features i.e. temporally aligned and unaligned respectively. As the temporally-aligned  
549 modality combinations of video-video and video-audio BLP fusion continue to succeed, we believe that  
550 the ‘natural alignment’ of modalities is a significant contributing factor to this performance discrepancy in  
551 video. To the best of our knowledge, we are the first to draw attention to this trend. Attention mechanisms  
552 continue to achieve state-of-the-art in video-language tasks and have been demonstrated (with visualisable

553 attention maps) to focus on relevant video and question features. We therefore recommend using attention  
554 mechanisms for their strong performance and relatively interpretable behaviour, and avoiding BLP for  
555 specifically video-text fusion.

556 **Empirically Justified on VQA:** Successive BLP techniques have helped drive increased VQA perfor-  
557 mance in recent years, as such they remain an important and welcome asset to the field of multimodal  
558 machine learning. We stress that these improvements, welcome as they are, are *only* justified by their  
559 empirical improvements in the tasks they are applied to, and lack strong theoretical frameworks which  
560 explain their superior performance. This is entirely understandable given the infamous difficulty in  
561 interpreting how neural networks *actually* make decisions or exploit their training data. However, it is  
562 often claimed that such improvements are the result of some intrinsic property of the BLP operator, e.g.  
563 creating ‘richer multimodal representations’: Fukui et al. (2016) *hypothesise* that concatenation is not  
564 as expressive as an outer product of visual and textual features. Kim et al. (2017) claim that “bilinear  
565 models provide rich representations compared with linear models”. Ben-younes et al. (2017) claim  
566 MUTAN “focuses on modelling fine and rich interactions between image and text modalities”. Yu et al.  
567 (2018b) claim that MFH significantly improves VQA performance “*because* they achieve more effective  
568 exploitation of the complex correlations between multimodal features”. Ben-Younes et al. (2019) carefully  
569 demonstrate that the extra control over the dimensions of components in BLOCK fusion can be leveraged  
570 to achieve yet higher VQA performance, however this is attributed to it’s ability “to represent very fine  
571 interactions between modalities while maintaining powerful mono-modal representations”. In contrast,  
572 Yu et al. (2017) carefully assess and discuss the *empirical* improvements their MFH fusion offers on VQA.  
573 Our discussions and findings highlight the importance of being measured and nuanced when discussing  
574 the theoretical nature of multimodal fusion techniques and the benefits they bring.

## 575 THEORETICALLY MOTIVATED OBSERVATIONS AND NEUROLOGICALLY 576 GUIDED PROPOSALS:

577 BLP techniques effectively exploit mathematical innovations on bilinear expansions represented in  
578 neural networks. As previously discussed, it remains unclear *why* any bilinear representation would be  
579 intrinsically superior for multimodal fusion to alternatives e.g. a series of non-linear fully connected layers  
580 or attention mechanisms. In this section, we share our thoughts on the properties of bilinear functions,  
581 and how they relate to neurological theories for multimodal processing in the human brain. We provide  
582 qualitative analysis of the distribution of psycholinguistic norms present in the video-QA datasets used in  
583 our experiments with which, through the lens of ‘Dual Coding Theory’ and the ‘Two-Stream’ model of  
584 vision, we propose neurologically motivated multimodal processing methodologies.

### 585 **Observations: Bilinearity in BLP**

586 **Nonlinearities in Bilinear Expansions:** As previously mentioned in our description of MLB, Kim et al.  
587 (2017) suggest using *Tanh* activation on the output of vector  $\mathbf{z}$  to further increase model capacity. Strictly  
588 speaking, we note that adding the the non-linearity means the representation is **no longer bilinear** as it is  
589 not linear with respect to either of its input domains. It is instead the ‘same kind of non-linear’ in both  
590 the input domains. We suggest that an alternative term such as ‘bi-nonlinear’ would more accurately  
591 described such functions. Bilinear representations are not the most complex functions with which to learn  
592 interactions between modalities. As explored by Yu et al. (2018b), we believe that higher-order interactions  
593 between features would facilitate a more realistic model of the world. The non-linear extension of bilinear  
594 or higher-order functions is a key factor to increase representational capacity.

595 **Outer Product Forces Multimodal Interactions:** The motivation for using bilinear methods over  
596 concatenation in VQA and video-QA was that it would enable learning more ‘complex’ or ‘expressive’  
597 interactions between the textual and visual inputs. We note however that concatenation of inputs features  
598 should theoretically allow both a weighted multimodal combination of textual and visual units, *and* allow  
599 unimodal units of input features. As visualised in Figure 9, weights representing a bilinear expansion  
600 in a neural network each represent a multiplication of input units from each modalitiy. This appears to,  
601 in some sense, *force* multimodal interactions where it could possibly be advantageous to allow some  
602 degree of separation between the text and vision modalities. As discussed earlier, it is thought that ‘joint’  
603 representations Baltrušaitis et al. (2019) preserve shared semantics while ignoring modality-specific  
604 information Guo et al. (2019). Though it is unclear if concatenation could effectively replicate bilinear  
605 processing while also preserving unimodal processing, it also remains unclear how *exactly* bilinear

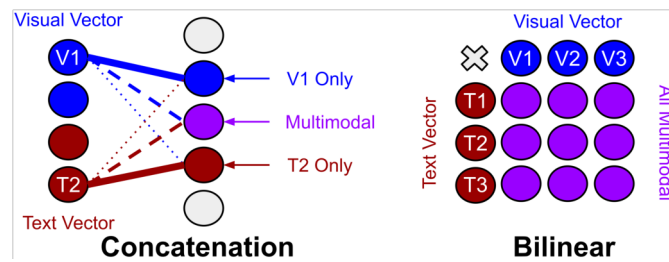


**Figure 9.** Visualisation of the differences between concatenation and bilinear representations for unimodal processing. Concatenation (left-A) can theoretically allow unimodal features from text or vision to process *independently* of the other modality by reducing its weighted contribution (see ‘V1 Only’). Bilinear representations (right-B) *force* multimodal interactions. It is less clear how useful ‘unimodal’ is processed.

606 representations learn. For now, the successes and struggles of bilinear representations across VQA and  
 607 video-QA remain justified by empirical performance on datasets.

### 608 **Proposals: Neurological Parallels**

609 We have recommended that video-QA models prioritise attention mechanisms over BLP given our own  
 610 experimental results and our observations of the current state-of-the-art trends. We *can* however still  
 611 explore how bilinear models in deep learning are related to 2 key areas of relevant neurological research,  
 612 i.e. the Two-Stream model of vision Goodale and Milner (1992); Milner (2017) and Dual Coding Theory  
 613 Paivio (2013, 2014).

614 **Two-Stream Vision:** Introduced in Goodale and Milner (1992), the current consensus on primate visual  
 615 processing is that it is divided into two networks or streams: The ‘ventral’ stream which mediates  
 616 transforming the contents of visual information into ‘mental furniture’ that guides memory, conscious  
 617 perception, and recognition; and the ‘dorsal’ stream which mediates the visual guidance of action. There  
 618 is a wealth of evidence showing that these two subsystems are not mutually insulated from each other, but  
 619 rather interconnect and contribute to one another at different stages of processing Milner (2017); Jeannerod  
 620 and Jacob (2005). In particular, Jeannerod and Jacob (2005) argue that valid comparisons between visual  
 621 representation must consider the direction of fit, direction of causation and the level of conceptual  
 622 content. They demonstrate that visual subsystems and behaviours inherently rely on aspects of both  
 623 streams. Recently, Milner (2017) consider 3 potential ways these cross-stream interactions could occur: **I**)  
 624 Computations along the 2 pathways are independent and combine at a ‘shared terminal’ (the independent  
 625 processing account), **II**) Processing along the separate pathways is modulated by feedback loops that  
 626 transfer information from ‘downstream’ brain regions, including information from the complementary  
 627 stream (the feedback account), **III**) Information is transferred between the 2 streams at multiple stages and  
 location along their pathways (the continuous cross-talk account). Though Milner (2017) focus mostly on

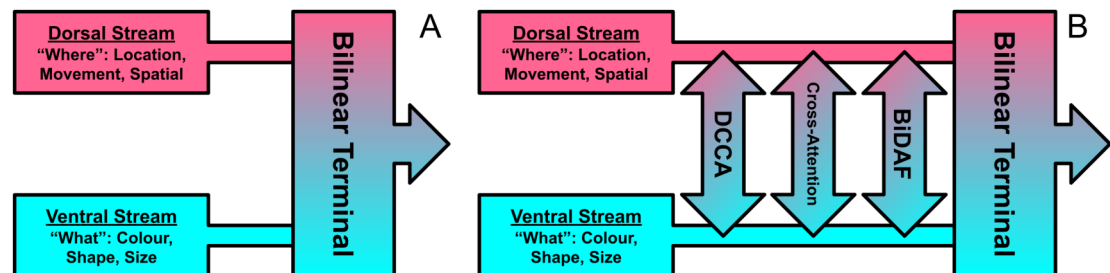


**Figure 10.** Visualisation of the 1<sup>st</sup> and 3<sup>rd</sup> cross-stream scenarios for the two-stream model of vision described by Milner (2017). The early bilinear model proposed by Tenenbaum and Freeman (2000) strikingly resembles the 1<sup>st</sup> (left-A). The 3<sup>rd</sup> and more recently favoured scenario features a continuous exchange of information across streams at multiple stages, and can be realised by introducing ‘cross-talking’ of deep learning features (right-B).

628

629 the ‘continuous cross-talk’ idea, they believe that a unifying theory would include aspects from each of  
 630 these scenarios. The vision-only deep bilinear models proposed in Tenenbaum and Freeman (2000); Lin  
 631 et al. (2015) are strikingly reminiscent to the 1<sup>st</sup> ‘shared-terminal’ scenario (see Figure 10). The bilinear  
 632 framework proposed in Tenenbaum and Freeman (2000) focuses on splitting up ‘style’ and ‘content’, and  
 633 is designed to be applied to any two-factor task. Lin et al. (2015) note but do not explore the similarities  
 634 between their proposed network and the two-stream model of vision. Their bilinear CNN model aims to  
 635 processes two subnetworks separately, ‘what’ (ventral) and ‘where’ (dorsal) streams, and later combine in  
 636 a bilinear ‘terminal’. BLP methods developed from these baselines would later focus on multimodal tasks  
 637 between language and vision. As Milner (2017) focus mainly on their 3<sup>rd</sup> scenario (right), subsequent  
 638 bilinear models that draw inspiration from the two-stream model of vision could realise the ‘cross-talk’  
 639 mechanism i.e. using co-attention or ‘co-ordinated’ DCCA.

640 **Dual Coding Theory:** Dual coding theory (DCT) Paivio (2013) broadly considers the interactions  
 641 between the verbal and non-verbal systems in the brain (recently surveyed in Paivio (2014)). DCT  
 642 considers verbal and non-verbal interactions by way of ‘logogens’ and ‘imagenes’ respectively, i.e. units  
 643 of verbal and non-verbal recognition. Imagenes may be multimodal, i.e. haptic, visual, smell, taste, motory  
 644 etc. We should appreciate the distinction between medium and modality: image is both medium and  
 645 modality and videos are an image based modality. Similarly, text is the medium through which the natural  
 646 language modality is expressed. We can see parallels in multimodal deep learning and dual coding theory,  
 647 with textual features as logogens and visual (or audio) features as visual (or auditory) imagenes. There are  
 648 many insights from DCT that could guide and drive multimodal deep learning:

649 **I)** Logogens and imagenes are discrete units of recognition and are often related to tangible concepts  
 650 (e.g. ‘pictogens’ Morton (1979)). By drawing inspiration from pictogen/imagen style of information  
 651 representation, it could be hypothesised that multimodal models should additionally focus on deriving  
 more tangible features (i.e. discrete convolution maps previously used in vision-only bilinear models Lin

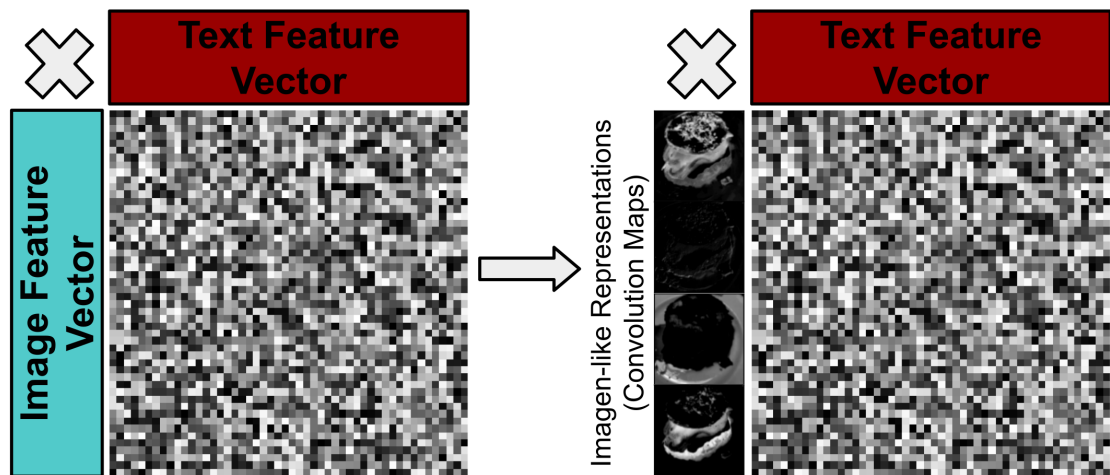


**Figure 11.** Visualisation of moving from less tangible visual features to more ‘imagen-like’ visual features e.g. convolution maps of an image.

652 et al. (2015)) as opposed to more abstracted ‘ImageNet-style’ feature vectors more commonly used in  
 653 recent BLP models (see Figure 11) are a more ideal way to represent features.

654 **II)** Bezemer and Kress (2008) explore the differences in student’s understanding when text information  
 655 is presented alongside other modalities. They argue that when meaning is moved from one medium to  
 656 another semiotic relations are redefined. This paradigm could be emulated to control how networks learn  
 657 concepts in relation to certain modal information.

658 **III)** Imagenes (and potentially logogens) may be a function of many modalities, i.e. one may recognise  
 659 something as a function of haptic and auditory experiences alongside visual ones. We believe this  
 660 implies that non-verbal modalities (vision/sound etc..) should be in some way grouped or aggregated, and  
 661 that while DCT remains widely accepted, multimodal research should consider ‘verbal vs non-verbal’  
 662 interactions as a whole instead of focusing too intently on ‘case-by-case’ interactions, i.e. text-vs-image  
 663 and text-vs-audio. This text/non-text insight may be related to the apparent difference in text-vision video  
 664

665 task performance previously discussed.

666 **IV) Multimodal cognitive behaviours in people can be improved by providing cues.** For example,  
667 referential processing (naming an object or identifying an object from a word) has been found to additively  
668 affect free recall (recite a list of items), with the memory contribution of non-verbal codes (pictures)  
669 being twice that of verbal codes Paivio and Lambert (1981). Begg (1972) find that free recall of ‘concrete  
670 phrases’ (can be visualised) of their constituent words is roughly twice that of ‘abstract’ phrases. However,  
671 this difference increased six-fold for concrete phrases when cued with one of the phrase words, yet  
672 using cues for abstract phrases did not help at all. This was named the ‘conceptual peg’ effect in DCT,  
673 and is interpreted as memory images being re-activated by ‘a high imagery retrieval cue’. Given such  
674 apparent differences in human cognitive processing for ‘concrete’ and ‘abstract’ words, it may similarly  
675 be beneficial for multimodal text-vision tasks to explicitly exploit the psycholinguistic ‘concreteness’  
676 word norm. Leveraging existing psycholinguistic word-norm datasets, we identify the relative abundance  
677 of concrete words in textual components of the video-QA datasets we experiment with (see Figure 12).  
678 As the various word-norm datasets use various scoring systems for concreteness (e.g. MTK40 uses a  
679 Likert scale 1-7), we rescale the scores for each dataset such that the lowest score is 0 (highly abstract),  
680 and the highest score is 1 (highly concrete). Though we cannot find a concreteness score for every word  
681 in each dataset component’s vocabulary, we see that the 4 video-QA datasets we experiment with have  
682 more concrete than abstract words overall. Furthermore, we see that answers are on-average significantly  
683 more concrete than they are abstract, and that (as intuitively expected) visual concepts from TVQA are  
684 even more concrete. Taking inspiration from human processing through DCT, it could be hypothesised  
685 that multimodal machine learning tasks could benefit by explicitly learning relations between ‘concrete’  
686 words and their constituents, whilst treating ‘abstract’ words and concepts differently.

687 Recently proposed computational models of DCT have had many drawbacks Paivio (2014), we believe  
688 that neural networks can be a natural fit for modelling neural correlates explored in DCT and should be  
689 considered as a future modelling option.

## 690 CONCLUSION

691 In light of BLP’s empirical success in VQA, we have experimentally explored their use in video-QA  
692 on 2 models and 4 datasets. We find that switching from vector concatenation to BLP through simple  
693 substitution on the HME and TVQA models does not improve and in fact actively harm performance on  
694 video-QA. We find that a more substantial ‘dual-stream’ restructuring of the TVQA model to accommodate  
695 BLP significantly reduces performance on TVQA. Our results and observations about the downturn in  
696 successful text-vision BLP fusion in video tasks imply that naively using BLP techniques can be very  
697 detrimental in video-QA. We caution against automatically integrating bilinear pooling in video-QA  
698 models and expecting similar empirical increases as in VQA. We offer several interpretations and insights  
699 of our negative results using surrounding multimodal and neurological literature and find our results  
700 inline with trends in VQA and video-classification. To the best of our knowledge, we are the first to  
701 outline how important neurological theories i.e. dual coding theory and the two-stream model of vision  
702 relate to the history of (and journey to) modern multimodal deep learning practices. We offer a few  
703 experimentally and theoretically guided suggestions to consider for multimodal fusion in video-QA, most  
704 notably that attention mechanisms should be prioritised over BLP in text-vision fusion. We qualitatively  
705 show the potential for neurologically-motivated multimodal approaches in video-QA by identifying the  
706 relative abundance of psycholinguistically ‘concrete’ words in the vocabularies for the text components  
707 of the 4 video-QA datasets we experiment with. We would like to emphasise the importance of related  
708 neurological theories in deep learning and encourage researchers to explore Dual Coding Theory and the  
709 Two-Stream model of vision.

## 710 ACKNOWLEDGMENTS

711 We would like to thank European Regional Development Fund, Stuart White, and Liz White for their  
712 support.

## 713 REFERENCES

714 Akaho, S. (2001). A kernel method for canonical correlation analysis. *Proceedings of the International*  
715 *Meeting of the Psychometric Society (IMPS 2001); Osaka, 4.*

- 716 Anderson, P., He, X., Buehler, C., Teney, D., Johnson, M., Gould, S., and Zhang, L. (2018). Bottom-up and  
717 top-down attention for image captioning and visual question answering. *2018 IEEE/CVF Conference*  
718 *on Computer Vision and Pattern Recognition*, pages 6077–6086.
- 719 Andrew, G., Arora, R., Bilmes, J. A., and Livescu, K. (2013). Deep canonical correlation analysis. In  
720 *ICML*.
- 721 Baltrušaitis, T., Ahuja, C., and Morency, L.-P. (2019). Multimodal machine learning: A survey and  
722 taxonomy. *IEEE Transactions on Pattern Analysis and Machine Intelligence*, 41:423–443.
- 723 Begg, I. (1972). Recall of meaningful phrases. *Journal of Verbal Learning and Verbal Behavior*,  
724 11(4):431–439.
- 725 Ben-younes, H., Cadène, R., Cord, M., and Thome, N. (2017). Mutan: Multimodal tucker fusion for  
726 visual question answering. *2017 IEEE International Conference on Computer Vision (ICCV)*, pages  
727 2631–2639.
- 728 Ben-Younes, H., Cadene, R., Thome, N., and Cord, M. (2019). Block: Bilinear superdiagonal fusion for  
729 visual question answering and visual relationship detection. In *Proceedings of the AAAI Conference on*  
730 *Artificial Intelligence*, volume 33, pages 8102–8109.
- 731 Bezemer, J. and Kress, G. (2008). Writing in multimodal texts: A social semiotic account of designs for  
732 learning. *Written Communication - WRIT COMMUN*, 25:166–195.
- 733 Brysbaert, M., Warriner, A., and Kuperman, V. (2013). Concreteness ratings for 40 thousand generally  
734 known english word lemmas. *Behavior research methods*, 46.
- 735 Charikar, M., Chen, K., and Farach-Colton, M. (2002). Finding frequent items in data streams. In  
736 Widmayer, P., Eidenbenz, S., Triguero, F., Morales, R., Conejo, R., and Hennessy, M., editors, *Automata,*  
737 *Languages and Programming*, pages 693–703, Berlin, Heidelberg. Springer Berlin Heidelberg.
- 738 Chen, D. L. and Dolan, W. B. (2011). Collecting highly parallel data for paraphrase evaluation. In *ACL*  
739 *2011*.
- 740 Chenyou, F. (2019). Hme-videoqa.
- 741 Chou, S.-H., Chao, W.-L., Sun, M., and Yang, M.-H. (2020). Visual question answering on 360° images.  
742 *2020 IEEE Winter Conference on Applications of Computer Vision (WACV)*, pages 1596–1605.
- 743 Clark, J. and Paivio, A. (2004). Extensions of the paivio, yuille, and madigan (1968) norms. <https://link.springer.com/article/10.3758/BF03195584#SecESM1>.
- 744
- 745 De Lathauwer, L. (2008a). Decompositions of a higher-order tensor in block terms—part i: Lemmas for  
746 partitioned matrices. *SIAM Journal on Matrix Analysis and Applications*, 30(3):1022–1032.
- 747 De Lathauwer, L. (2008b). Decompositions of a higher-order tensor in block terms—part ii: Definitions  
748 and uniqueness. *SIAM Journal on Matrix Analysis and Applications*, 30(3):1033–1066.
- 749 De Lathauwer, L. and Nion, D. (2008). Decompositions of a higher-order tensor in block terms—part iii:  
750 Alternating least squares algorithms. *SIAM journal on Matrix Analysis and Applications*, 30(3):1067–  
751 1083.
- 752 Deb, T., Sadmanee, A., Bhaumik, K. K., Ali, A. M., Amin, M. A., and Rahman, A. K. M. M. (2022).  
753 Variational stacked local attention networks for diverse video captioning. *2022 IEEE/CVF Winter*  
754 *Conference on Applications of Computer Vision (WACV)*, pages 2493–2502.
- 755 Deng, H., Kong, J., Jiang, M., and Liu, T. (2021). Diverse features fusion network for video-based action  
756 recognition. *Journal of Visual Communication and Image Representation*, 77:103121.
- 757 Deng, J., Dong, W., Socher, R., Li, L., Kai Li, and Li Fei-Fei (2009). Imagenet: A large-scale hierarchical  
758 image database. In *2009 IEEE Conference on Computer Vision and Pattern Recognition*, pages  
759 248–255.
- 760 Devlin, J., Chang, M.-W., Lee, K., and Toutanova, K. (2019). Bert: Pre-training of deep bidirectional  
761 transformers for language understanding. In *NAACL-HLT*.
- 762 Domínguez, A. (2015). A history of the convolution operation [retrospectroscope]. *IEEE Pulse*, 6(1):38–  
763 49.
- 764 Fan, C. (2019). Egovqa - an egocentric video question answering benchmark dataset. In *The IEEE*  
765 *International Conference on Computer Vision (ICCV) Workshops*.
- 766 Fan, C., Zhang, X., Zhang, S., Wang, W., Zhang, C., and Huang, H. (2019). Heterogeneous memory  
767 enhanced multimodal attention model for video question answering. In *2019 IEEE/CVF Conference on*  
768 *Computer Vision and Pattern Recognition (CVPR)*, pages 1999–2007, Los Alamitos, CA, USA. IEEE  
769 Computer Society.
- 770 Friendly, M., Franklin, P., Hoffman, D., and Rubin, D. (1982). The toronto word pool: Norms for imagery,

- 771 concreteness, orthographic variables, and grammatical usage for 1,080 words. *Behavior Research*  
772 *Methods & Instrumentation*, 14:375–399.
- 773 Fukui, A., Park, D. H., Yang, D., Rohrbach, A., Darrell, T., and Rohrbach, M. (2016). Multimodal  
774 compact bilinear pooling for visual question answering and visual grounding. In *Proceedings of the*  
775 *2016 Conference on Empirical Methods in Natural Language Processing*, pages 457–468, Austin,  
776 Texas. Association for Computational Linguistics.
- 777 Gao, J., Ge, R., Chen, K., and Nevatia, R. (2018). Motion-appearance co-memory networks for video  
778 question answering. *2018 IEEE/CVF Conference on Computer Vision and Pattern Recognition*, pages  
779 6576–6585.
- 780 Gao, L., Zeng, P., Song, J., Li, Y.-F., Liu, W., Mei, T., and Shen, H. T. (2019). Structured two-stream  
781 attention network for video question answering. In *AAAI*.
- 782 Gao, Y., Beijbom, O., Zhang, N., and Darrell, T. (2016). Compact bilinear pooling. In *2016 IEEE*  
783 *Conference on Computer Vision and Pattern Recognition (CVPR)*, pages 317–326.
- 784 Goodale, M. A. (2014). How (and why) the visual control of action differs from visual perception.  
785 *Proceedings of the Royal Society B: Biological Sciences*, 281(1785):20140337.
- 786 Goodale, M. A. and Milner, A. D. (1992). Separate visual pathways for perception and action. *Trends in*  
787 *neurosciences*, 15(1):20–25.
- 788 Graves, A. and Schmidhuber, J. (2005). Frameworkwise phoneme classification with bidirectional lstm and  
789 other neural network architectures. *Neural Networks*, 18(5-6):602–610.
- 790 Guadarrama, S., Krishnamoorthy, N., Malkarnenkar, G., Venugopalan, S., Mooney, R. J., Darrell, T.,  
791 and Saenko, K. (2013). Youtube2text: Recognizing and describing arbitrary activities using semantic  
792 hierarchies and zero-shot recognition. *2013 IEEE International Conference on Computer Vision*, pages  
793 2712–2719.
- 794 Guillaume OLIKIER, Pierre-Antoine ABSIL, L. D. L. (2017). Tensor approximation by block term  
795 decomposition. *Dissertation*.
- 796 Guo, W., Wang, J., and Wang, S. (2019). Deep multimodal representation learning: A survey. *IEEE*  
797 *Access*, 7:63373–63394.
- 798 Guo, Z., Zhao, J., Jiao, L., Liu, X., and Li, L. (2021). Multi-scale progressive attention network for video  
799 question answering. In *Proceedings of the 59th Annual Meeting of the Association for Computational*  
800 *Linguistics*.
- 801 He, K., Zhang, X., Ren, S., and Sun, J. (2016). Deep residual learning for image recognition. *2016 IEEE*  
802 *Conference on Computer Vision and Pattern Recognition (CVPR)*, pages 770–778.
- 803 Heilman, M. and Smith, N. A. (2009). Question generation via overgenerating transformations and  
804 ranking. In *CMU*.
- 805 Hill, F., Reichart, R., and Korhonen, A. (2015). SimLex-999: Evaluating semantic models with (genuine)  
806 similarity estimation. *Computational Linguistics*, 41(4):665–695.
- 807 Hochreiter, S. and Schmidhuber, J. (1997). Long short-term memory. *Neural Comput.*, 9(8):1735–1780.
- 808 Hotelling, H. (1936). Relations between two sets of variates. *Biometrika*, 28(3/4):321–377.
- 809 Hu, F., Mohedano, E., O’Connor, N. E., and McGuinness, K. (2021). Temporal bilinear encoding network  
810 of audio-visual features at low sampling rates. In *VISIGRAPP*.
- 811 Isola, P., Lim, J. J., and Adelson, E. H. (2015). Discovering states and transformations in image collections.  
812 *2015 IEEE Conference on Computer Vision and Pattern Recognition (CVPR)*, pages 1383–1391.
- 813 Jang, Y., Song, Y., Yu, Y., Kim, Y., and Kim, G. (2017). TGIF-QA: Toward Spatio-Temporal Reasoning  
814 in Visual Question Answering. In *CVPR*.
- 815 Jeannerod, M. and Jacob, P. (2005). Visual cognition: a new look at the two-visual systems model.  
816 *Neuropsychologia*, 43(2):301–312.
- 817 Karpathy, A. and Fei-Fei, L. (2015). Deep visual-semantic alignments for generating image descriptions.  
818 In *CVPR*.
- 819 Khan, A. U., Mazaheri, A., Lobo, N., and Shah, M. (2020). Mmft-bert: Multimodal fusion transformer  
820 with bert encodings for visual question answering. In *FINDINGS*.
- 821 Kim, J., Ma, M., Kim, K., Kim, S., and Yoo, C. (2019). Progressive attention memory network for movie  
822 story question answering. *2019 IEEE/CVF Conference on Computer Vision and Pattern Recognition*  
823 *(CVPR)*, pages 8329–8338.
- 824 Kim, J., On, K. W., Lim, W., Kim, J., Ha, J., and Zhang, B. (2017). Hadamard product for low-rank  
825 bilinear pooling. *ICLR*.

- 826 Krishna, R., Zhu, Y., Groth, O., Johnson, J., Hata, K., Kravitz, J., Chen, S., Kalantidis, Y., Li, L.-J.,  
827 Shamma, D. A., Bernstein, M. S., and Fei-Fei, L. (2017). Visual genome: Connecting language and  
828 vision using crowdsourced dense image annotations. *Int. J. Comput. Vision*, 123(1):32–73.
- 829 Le, H., Sahoo, D., Chen, N. F., and Hoi, S. (2020). Bist: Bi-directional spatio-temporal reasoning for  
830 video-grounded dialogues. In *EMNLP*.
- 831 Lei, J., Li, L., Zhou, L., Gan, Z., Berg, T. L., Bansal, M., and Liu, J. (2021). Less is more: Clipbert for  
832 video-and-language learning via sparse sampling. In *CVPR*.
- 833 Lei, J., Yu, L., Bansal, M., and Berg, T. L. (2018). Tvqa: Localized, compositional video question  
834 answering. In *EMNLP*.
- 835 Levy, O. and Wolf, L. (2015). Live repetition counting. *2015 IEEE International Conference on Computer  
836 Vision (ICCV)*, pages 3020–3028.
- 837 Li, X., Gao, L., Wang, X., Liu, W., Xu, X., Shen, H. T., and Song, J. (2019). Learnable aggregating  
838 net with diversity learning for video question answering. *Proceedings of the 27th ACM International  
839 Conference on Multimedia*.
- 840 Li, Y., Song, Y., Cao, L., Tetreault, J. R., Goldberg, L., Jaimes, A., and Luo, J. (2016). Tgif: A new  
841 dataset and benchmark on animated gif description. *2016 IEEE Conference on Computer Vision and  
842 Pattern Recognition (CVPR)*, pages 4641–4650.
- 843 Liang, J., Jiang, L., Cao, L., Kalantidis, Y., Li, L., and Hauptmann, A. (2019). Focal visual-text attention  
844 for memex question answering. *IEEE Transactions on Pattern Analysis and Machine Intelligence*,  
845 41:1893–1908.
- 846 Lin, T., RoyChowdhury, A., and Maji, S. (2015). Bilinear cnn models for fine-grained visual recognition.  
847 In *2015 IEEE International Conference on Computer Vision (ICCV)*, pages 1449–1457.
- 848 Liu, F., Liu, J., Hong, R., and Lu, H. (2021). Question-guided erasing-based spatiotemporal attention  
849 learning for video question answering. *IEEE Transactions on Neural Networks and Learning Systems*.
- 850 Ljubešić, N., Fišer, D., and Peti-Stantić, A. (2018). Predicting concreteness and imageability of words  
851 within and across languages via word embeddings. In *Proceedings of the 3rd Workshop on Representa-  
852 tion Learning for NLP, ReL4NLP@ACL 2018, Melbourne, Australia, July 20, 2018*.
- 853 Long, X., Gan, C., de Melo, G., Liu, X., Li, Y., Li, F., and Wen, S. (2018). Multimodal keyless attention  
854 fusion for video classification. In *AAAI*.
- 855 Lu, J., Yang, J., Batra, D., and Parikh, D. (2016). Hierarchical question-image co-attention for visual  
856 question answering. In *Proceedings of the 30th International Conference on Neural Information  
857 Processing Systems, NIPS' 16*, page 289–297. Curran Associates Inc.
- 858 Milner, A. D. (2017). How do the two visual streams interact with each other? *Experimental Brain  
859 Research*, 235:1297 – 1308.
- 860 Milner, A. D. and Goodale, M. A. (2008). Two visual systems re-viewed. *Neuropsychologia*, 46(3):774–  
861 785.
- 862 Milner, D. and Goodale, M. (2006). *The visual brain in action*, volume 27. OUP Oxford.
- 863 Morton, J. (1979). *Facilitation in Word Recognition: Experiments Causing Change in the Logogen Model*,  
864 pages 259–268. Springer US, Boston, MA.
- 865 Nelson, D., Mcevoy, C., and Schreiber, T. (1998). The university of south florida word association, rhyme,  
866 and word fragment norms. <http://w3.usf.edu/FreeAssociation/>.
- 867 Osman, A. and Samek, W. (2019). Drau: Dual recurrent attention units for visual question answering.  
868 *Computer Vision and Image Understanding*, 185:24–30.
- 869 Paivio, A. (2013). *Imagery and verbal processes*. Psychology Press.
- 870 Paivio, A. (2014). Intelligence, dual coding theory, and the brain. *Intelligence*, 47:141–158.
- 871 Paivio, A. and Lambert, W. (1981). Dual coding and bilingual memory. *Journal of Verbal Learning and  
872 Verbal Behavior*, 20(5):532–539.
- 873 Pang, W.-F., He, Q.-H., Hu, Y.-j., and Li, Y.-X. (2021). Violence detection in videos based on fusing  
874 visual and audio information. In *ICASSP 2021 - 2021 IEEE International Conference on Acoustics,  
875 Speech and Signal Processing (ICASSP)*, pages 2260–2264.
- 876 Peng, Y., Qi, J., and Yuan, Y. (2018). Modality-specific cross-modal similarity measurement with recurrent  
877 attention network. *IEEE Transactions on Image Processing*, 27:5585–5599.
- 878 Pennington, J., Socher, R., and Manning, C. D. (2014). Glove: Global vectors for word representation. In  
879 *Empirical Methods in Natural Language Processing (EMNLP)*, pages 1532–1543.
- 880 Reilly, J. and Kean, J. (2007). Formal distinctiveness of high- and low-imageability nouns: Analyses and

- 881 theoretical implications. *Cognitive science*, 31:157–68.
- 882 Ren, S., He, K., Girshick, R., and Sun, J. (2015). Faster r-cnn: Towards real-time object detection with  
883 region proposal networks. In Cortes, C., Lawrence, N., Lee, D., Sugiyama, M., and Garnett, R., editors,  
884 *Advances in Neural Information Processing Systems*, volume 28. Curran Associates, Inc.
- 885 Scott, G. G., Keitel, A., Becirspahic, M., O'Donnell, P. J., and Sereno, S. C. (2017). The glasgow norms:  
886 Ratings of 5,500 words on 9 scales.
- 887 Seo, A., Kang, G.-C., Park, J., and Zhang, B.-T. (2021). Attend what you need: Motion-appearance  
888 synergistic networks for video question answering. In *ACL/IJCNLP*.
- 889 Seo, M., Kembhavi, A., Farhadi, A., and Hajishirzi, H. (2017). Bidirectional attention flow for machine  
890 comprehension. *ICLR*.
- 891 Sianipar, A., Groenestijn, P., and Dijkstra, T. (2016). Affective meaning, concreteness, and subjective  
892 frequency norms for indonesian words. *Frontiers in Psychology*, 7:1907.
- 893 Simonyan, K. and Zisserman, A. (2015). Very deep convolutional networks for large-scale image  
894 recognition. In *International Conference on Learning Representations*.
- 895 Srivastava, Y., Murali, V., Dubey, S. R., and Mukherjee, S. (2020). Visual question answering using deep  
896 learning: A survey and performance analysis. *CVIP*.
- 897 Sudhakaran, S., Escalera, S., and Lanz, O. (2021). Learning to recognize actions on objects in egocentric  
898 video with attention dictionaries. *IEEE transactions on pattern analysis and machine intelligence*, PP.
- 899 Sukhbaatar, S., Szlam, A., Weston, J., and Fergus, R. (2015). End-to-end memory networks. In *NIPS*.
- 900 Sun, G., Liang, L., Li, T., Yu, B., Wu, M., and Zhang, B. (2021). Video question answering: a survey of  
901 models and datasets. *Mobile Networks and Applications*, pages 1–34.
- 902 Tapaswi, M., Zhu, Y., Stiefelwagen, R., Torralba, A., Urtasun, R., and Fidler, S. (2016). MovieQA:  
903 Understanding Stories in Movies through Question-Answering. In *IEEE Conference on Computer  
904 Vision and Pattern Recognition (CVPR)*.
- 905 Tenenbaum, J. B. and Freeman, W. T. (2000). Separating style and content with bilinear models. *Neural  
906 Comput.*, 12(6):1247–1283.
- 907 Tran, D., Bourdev, L. D., Fergus, R., Torresani, L., and Paluri, M. (2014). C3d: Generic features for video  
908 analysis. *ArXiv*, abs/1412.0767.
- 909 Tucker, L. R. (1966). Some mathematical notes on three-mode factor analysis. *Psychometrika*, 31(3):279–  
910 311.
- 911 Wang, J., Bao, B., and Xu, C. (2021). Dualvgr: A dual-visual graph reasoning unit for video question  
912 answering. *IEEE Transactions on Multimedia*.
- 913 Winterbottom, T., Xiao, S., McLean, A., and Al Moubayed, N. (2020). On modality bias in the tvqa  
914 dataset. In *Proceedings of the British Machine Vision Conference (BMVC)*.
- 915 Wu, Q., Teney, D., Wang, P., Shen, C., Dick, A. R., and van den Hengel, A. (2017). Visual question  
916 answering: A survey of methods and datasets. *Comput. Vis. Image Underst.*, 163:21–40.
- 917 Xiong, C., Merity, S., and Socher, R. (2016). Dynamic memory networks for visual and textual question  
918 answering. In *ICML*.
- 919 Xu, D., Zhao, Z., Xiao, J., Wu, F., Zhang, H., He, X., and Zhuang, Y. (2017). Video question answering  
920 via gradually refined attention over appearance and motion. *Proceedings of the 25th ACM international  
921 conference on Multimedia*.
- 922 Xu, Q., Mei, Y., Liu, J., and Li, C. (2021). Multimodal cross-layer bilinear pooling for rgbt tracking.  
923 *IEEE Transactions on Multimedia*, pages 1–1.
- 924 Yang, A., Miech, A., Sivic, J., Laptev, I., and Schmid, C. (2021). Just ask: Learning to answer questions  
925 from millions of narrated videos. In *Proceedings of the IEEE/CVF International Conference on  
926 Computer Vision (ICCV)*, pages 1686–1697.
- 927 Ye, Y., Zhao, Z., Li, Y., Chen, L., Xiao, J., and Zhuang, Y. (2017). Video question answering via  
928 attribute-augmented attention network learning. *Proceedings of the 40th International ACM SIGIR  
929 Conference on Research and Development in Information Retrieval*.
- 930 Yee, L. T. S. (2017). Valence, arousal, familiarity, concreteness, and imageability ratings for 292  
931 two-character chinese nouns in cantonese speakers in hong kong. *PLoS ONE*, 12.
- 932 Yin, X. and Ordonez, V. (2017). Obj2text: Generating visually descriptive language from object layouts.  
933 In *EMNLP*.
- 934 Yu, A. W., Dohan, D., Luong, M., Zhao, R., Chen, K., Norouzi, M., and Le, Q. V. (2018a). Qanet:  
935 Combining local convolution with global self-attention for reading comprehension. *ICLR*.

- 936 Yu, Z., Yu, J., Fan, J., and Tao, D. (2017). Multi-modal factorized bilinear pooling with co-attention  
937 learning for visual question answering. In *Proceedings of the IEEE international conference on*  
938 *computer vision*, pages 1821–1830.
- 939 Yu, Z., Yu, J., Xiang, C., Fan, J., and Tao, D. (2018b). Beyond bilinear: Generalized multimodal factorized  
940 high-order pooling for visual question answering. *IEEE Transactions on Neural Networks and Learning*  
941 *Systems*, 29:5947–5959.
- 942 Zeng, K.-H., Chen, T.-H., Chuang, C.-Y., Liao, Y.-H., Niebles, J. C., and Sun, M. (2017). Leveraging  
943 video descriptions to learn video question answering. *ArXiv*, abs/1611.04021.
- 944 Zhou, B., Tian, Y., Sukhbaatar, S., Szlam, A., and Fergus, R. (2015). Simple baseline for visual question  
945 answering. *ArXiv*, abs/1512.02167.
- 946 Zhou, H., Du, J., Zhang, Y., Wang, Q., Liu, Q.-F., and Lee, C.-H. (2021). Information fusion in attention  
947 networks using adaptive and multi-level factorized bilinear pooling for audio-visual emotion recognition.  
948 *IEEE/ACM Transactions on Audio, Speech, and Language Processing*, 29:2617–2629.

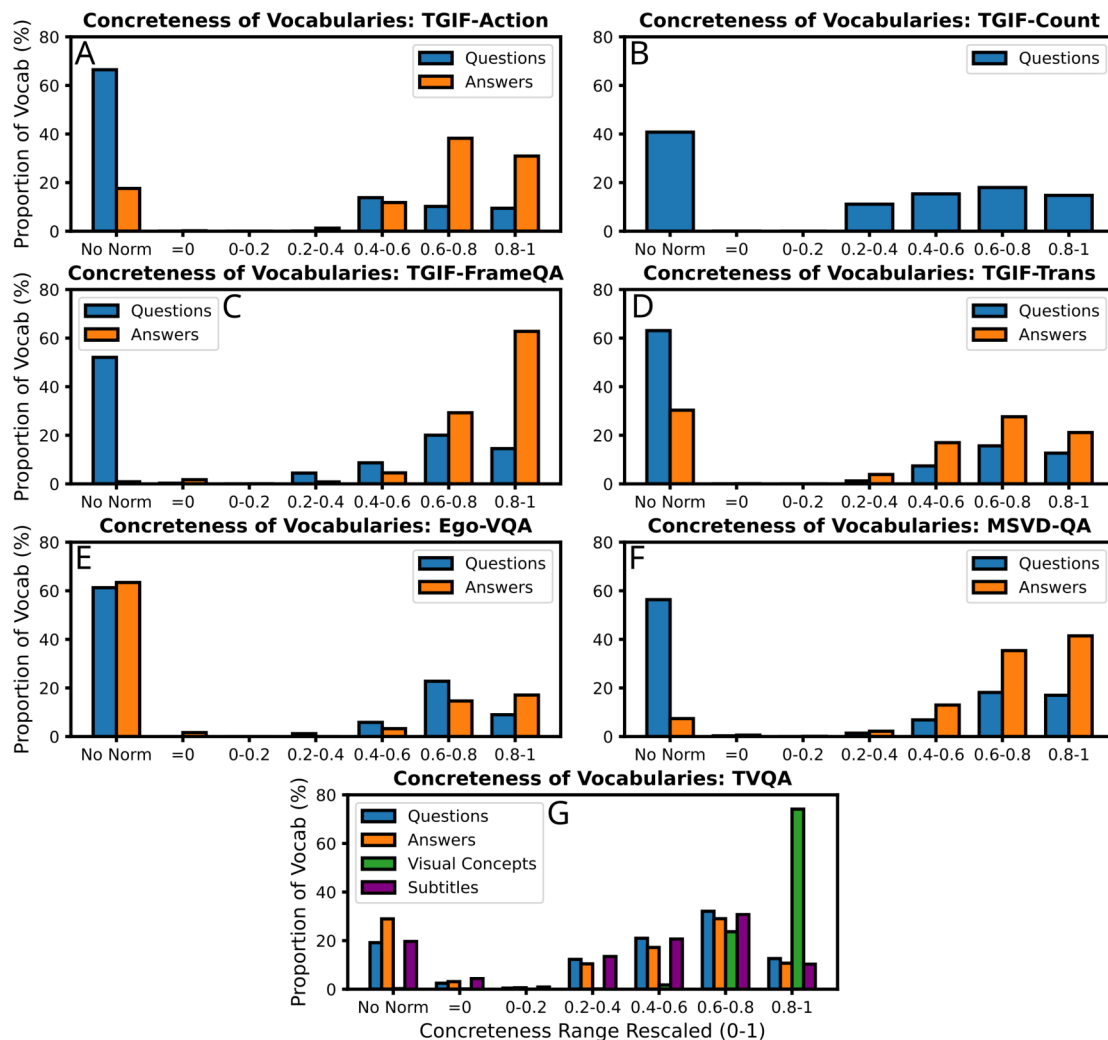


**Figure 12.** The relative abundance of the psycholinguistic ‘concreteness’ score in the *vocabularies* of each source of text in the video-QA datasets we experiment with. Stopwords are not included. Concreteness scores are taken from the following datasets: MT40k Brysbaert et al. (2013), USF Nelson et al. (1998), SimLex999 Hill et al. (2015), Clark-Paivio Clark and Paivio (2004), Toronto Word Pool Friendly et al. (1982), Chinese Word Norm Corpus Yee (2017), MEGHR-Crossling Ljubešić et al. (2018), Glasgow Norms Scott et al. (2017), Reilly and Kean (2007), and Sianipar et al. (2016). The scores for each word are rescaled from 0-1 such that most abstract = 0 and most concrete = 1, and the result averaged if more than 1 dataset has the same word.